Weierstraß-Institut
für Angewandte Analysis und Stochastik
Leibniz-Institut im Forschungsverbund Berlin e. V.

Preprint ISSN 2198-5855

Joint model of probabilistic-robust (probust) constraints with application to gas network optimization

Dennis Adelhütte[1], Denis Aßmann[1], Tatiana González Grandón[2], Martin Gugat[1], Holger Heitsch[3], René Henrion[3], Frauke Liers[1], Sabrina Nitsche[4], Rüdiger Schultz[4], Michael Stingl[1], David Wintergerst[1]

submitted: November 14, 2018

[1] Friedrich-Alexander-Universität Erlangen-Nürnberg
Cauerstr. 11
91058 Erlangen, Germany
E-Mail: frauke.liers@fau.de

[2] Institute of Mathematics
Humboldt-Universität zu Berlin
Unter den Linden 6
10099 Berlin, Germany
E-Mail: gonzalet@hu-berlin.de

[3] Weierstrass Institute
Mohrenstr. 39
10117 Berlin, Germany
E-Mail: holger.heitsch@wias-berlin.de
rene.henrion@wias-berlin.de

[4] University of Duisburg-Essen
Faculty of Mathematics
Thea-Leymann-Str. 9
45127 Essen, Germany
E-Mail: ruediger.schultz@uni-due.de

No. 2550
Berlin 2018

2010 *Mathematics Subject Classification.* 90B15, 90C15, 90C26, 93D15, 93D21.

Key words and phrases. Stabilization, wave equation, feedback, robust optimization, probabilistic constraints, probust, Karhunen-Loève.

This work is supported by the DFG within the projects B04, B05, B06 and C03 of CRC TRR 154.

Edited by
Weierstraß-Institut für Angewandte Analysis und Stochastik (WIAS)
Leibniz-Institut im Forschungsverbund Berlin e. V.
Mohrenstraße 39
10117 Berlin
Germany

Fax: +49 30 20372-303
E-Mail: preprint@wias-berlin.de
World Wide Web: http://www.wias-berlin.de/

Joint model of probabilistic-robust (probust) constraints with application to gas network optimization

Dennis Adelhütte, Denis Aßmann , Tatiana González Grandón, Martin Gugat , Holger Heitsch, René Henrion , Frauke Liers , Sabrina Nitsche, Rüdiger Schultz , Michael Stingl , David Wintergerst

Abstract

Optimization problems under uncertain conditions abound in many real-life applications. While solution approaches for probabilistic constraints are often developed in case the uncertainties can be assumed to follow a certain probability distribution, robust approaches are usually applied in case solutions are sought that are feasible for all realizations of uncertainties within some predefined uncertainty set. As many applications contain different types of uncertainties that require robust as well as probabilistic treatments, we introduce a class of joint probabilistic/robust constraints. Focusing on complex uncertain gas network optimization problems, we show the relevance of this class of problems for the task of maximizing free booked capacities in an algebraic model for a stationary gas network. We furthermore present approaches for finding their solution. Finally, we study the problem of controlling a transient system that is governed by the wave equation. The task consists in determining controls such that a certain robustness measure remains below some given upper bound with high probability.

1 Introduction

1.1 Joint probabilistic/robust constraints

Decision making problems are more than often affected by parameter uncertainty. An optimization problem dealing with uncertain variables has the typical form

$$\begin{array}{ll} \min\limits_{x} & g_0(x) \\ \text{subject to} & g_i(x,z) \geq 0 \quad (i=1,\ldots,k) \end{array} \tag{1}$$

Here $x \in \mathbb{R}^n$ is a decision vector, $z \in \mathbb{R}^m$ is an uncertain parameter, $g_0 \colon \mathbb{R}^n \to \mathbb{R}$ is the objective function and $g \colon \mathbb{R}^n \times \mathbb{R}^m \to \mathbb{R}^k$ is the constraint mapping. The decision support schemes with non-deterministic parameters have to take into account the nature and source of uncertainty while balancing the objective and the constraints of the problem. There are two main approaches for dealing with uncertainty in the constraints of an optimization problem: the first one is the use of *probabilistic constraints*. This approach is based on the assumption that historical data is available to estimate the probability distribution of the uncertain parameter and thus considering it as a random vector ξ. Then (1) may be given the form

$$\begin{array}{ll} \min\limits_{x} & g_0(x) \\ \text{subject to} & \mathbb{P}\big(g(x,\xi) \geq 0\big) \geq p \in (0,1] \end{array} \tag{2}$$

DOI 10.20347/WIAS.PREPRINT.2550 Berlin 2018

(note that the first '$\geq$' sign is to be understood component-wise). Here, a decision x is declared to be feasible if and only if the original random inequality system (1) is satisfied with a prescribed probability p, a level usually chosen close to but not identical to one. Of course, higher values of p lead to smaller set of feasible decisions x in (2), hence to optimal solutions at higher costs. For a standard reference on optimization problems with probabilistic constraints we refer to the monograph [24].

An alternative approach is given by *robust optimization*. It applies when the uncertain parameter u is completely unknown or non-stochastic due to a lack of available data. Then, satisfaction of the uncertain inequality system (1) is required for every realization of the uncertainty parameter within some uncertainty set $\mathcal{U} \subseteq \mathbb{R}^m$, so that one arrives at the following optimization problem:

$$\begin{array}{ll} \min\limits_{x} & g_0(x) \\ \text{subject to} & g(x,u) \geq 0 \quad \forall u \in \mathcal{U} \end{array} \tag{3}$$

For a basic monograph on robust optimization, we refer to [4].

We notice that both optimization models with probabilistic and robust constraints are deterministic reformulations of (1), since they depend only on the decision vector x but no longer on the outcome of the uncertain parameter z.

A central issue in robust optimization is the appropriate choice of the uncertainty set $\mathcal{U}$. Simple-shaped sets like polyhedra or ellipsoids induce computationally tractability and allow one to deal with much larger dimensions than in the case of probabilistic constraints. Moreover, when choosing $\mathcal{U}$ such that $\mathbb{P}(\xi \in \mathcal{U}) = p$, then the feasible set of decision variables x of (3) is contained in that of probabilistic programming (2), so that an optimal solution to (3) is a feasible solution to (2). For these two reasons, robust optimization is not only preferred in the absence of statistical data, but also as a conservative approximation of the probabilistic programming setting. This conservatism, however, may be significant up to the point of ending up at very small or even empty feasible sets possibly coming at much higher costs than under a probabilistic constraints. This trade-off propels the use of probabilistic constraints in the presence of statistical information at least in moderate dimension.

Although these approaches, probabilistic programming and robust optimization are often dealt with separately, in many applications, one is faced with uncertain variables of both mentioned types. This leads us naturally to the consideration of uncertain inequalities (2) in which the uncertain variable has a stochastic and a non-stochastic part, i.e., $z = (\xi, u)$. A typical example is optimization of gas transport in the presence of uncertain loads, for which historical data are available in many situations (stochastic uncertainty) and of uncertain roughness coefficients in pipes, for which observations can hardly be accessed (non-stochastic uncertainty). Therefore, it seems natural, to combine the originally separate models (2) and (3). An appropriate way to do so is to formulate a probabilistic constraint (w.r.t. ξ) involving a robustified (w.r.t. u) infinite inequality system:

$$\mathbb{P}\big(g(x,\xi,u) \geq 0 \quad \forall u \in \mathcal{U}\big) \geq p. \tag{4}$$

This class of constraints has been recently investigated in [1] under the name of *hybrid robust/chance-constraints* and in [12] under the name of *probabilistic/robust constraints*. For easier reference, we shall be using in the following the natural acronym of *probust constraints*. We note that even the more complex situation of the uncertainty set depending on the decision and random variable plays an increasing role in applications. Here, the constraint becomes

$$\mathbb{P}\big(g(x,\xi,u) \geq 0 \quad \forall u \in \mathcal{U}(x,\xi)\big) \geq p \tag{5}$$

where the inner part resembles constraint sets arising in generalized semi-infinite optimization [25].

We note that yet another form of combining the probabilistic and robust parts of the inequality system would result from interchanging their arrangements in (4) :

$$\mathbb{P}\big(g(x,\xi,u)\geq 0\big)\geq p \quad \forall u\in\mathcal{U}$$

In this way one does not arrive at a probabilistic constraint involving infnitely many random inequalities as in (4) but rather at an infinite system of probabilitic constraints. This setting is related to (robust) first-order stochastic dominance constraints [7] and to distributionally robust probabilistic constraints [26], which currently receive increased attention. We won't deal with this model here but rather focus our considerations on (4) and (5) respectively.

The aim of this paper is to illustrate the application of this new class of probust constraints to optimization problems in gas transport under uncertainty. For a recent monograph on gas transport optimization we refer to [20]. We will consider first the problem of maximizing free booked capacities in an algebraic model for a stationary gas network. The corresponding model is presented in Section 2. This overall problem is too complex, however, to be dealt within this paper. Therefore we will split it into two subproblems, namely capacity maximization at exits (consumer side) which is discussed in Section 3 and capacity maximization at entries (provider side) which is analyzed in Section 4. Without loss of generality, we follow the convention of entry loads being non positive and exit loads being non negative.

In contrast to the first two parts of the paper, where stationary problems are studied, in the second application in Section 5, we consider a transient system. The transient system is governed by the wave equation under probabilistic initial and Dirichlet boundary data at one end of the space interval. At the other end of the space interval Neumann velocity feedback is active. For the system a desired stationary state is given. The robustness of the system is measured by the L^∞-norm of the difference between the actual state $\tilde{v}$ and the desired state $\bar{v}$. Due to the definition of the L^∞-norm (as the essential supremum of the absolute value), this approach gives information about the maximal pointwise distance in space and time. Since our solutions are in fact continuous for appropriate initial and boundary data, the L^∞- norm is equal to the maximum norm. The robustness requirement is that this pointwise distance remains below a given upper bound $v_{\max}$. In our system, the state depends on uncertain initial and boundary data with a given probability distribution. The probabilistic constraint requires that the probability that the robustness requirement is satisfied is sufficiently large, i.e. greater or equal to a given value $p\in(0,1]$. This probabilistic constraint can be written in the form of (4); for details see Section 5, Eq. (38). As a numerical example, we consider the optimization with respect to the feedback parameter in Subsection 5.3.

2 Maximization of free capacities in a stationary network

We consider a passive stationary gas network given by a directed graph $\mathcal{G}=(V,E)$ with a set V of vertices and a set E of edges. We shall assume that the set of nodes decomposes into a set V_+ of entries, where gas is injected and a set V_- of exits, where gas is withdrawn. Hence, $V=V_+\cup V_-$ and $V_+\cap V_-=\emptyset$. Without loss of generality we label the nodes in a way that entries come first and exits last. The gas transport along the network is triggered by bilateral delivery contracts between traders who inject gas at entries and traders covering customer demands by withdrawing gas at exits. An amount of gas injected into or withdrawn from the network at certain nodes is called a nomination. We shall refer to $b\leq 0$ and $\xi\geq 0$ as to the vectors of nominations at entries and exits, respectively.

Nominations have to satisfy three conditions:

1 At each node (entry or exit) of the network, nominations must not exceed the capacity booked for that node by the respective trader.

2 Nominations must be balanced over the whole network, i.e., the sum of nominations at entries equals the sum of nominations at exits.

3 Nominations must be technically feasible in the sense that there exist pressures within given bounds at the nodes and a flow through the network such that the nominations at the exits can be served by the nominations at the entries.

The first condition has to be satisfied by the traders. Referring to $C_-, C_+ \geq 0$ as to the vectors of booked capacities at entries and exits, respectively, it can be written as

$$b \in [-C_+, 0]\,,\ \xi \in [0, C_-]\,, \tag{6}$$

where the intervals are to be understood in a multidimensional sense. The second condition is an automatic consequence of the ensemble of bilateral delivery contracts between entries and exits and can be written as

$$\mathbf{1}_+^T b + \mathbf{1}_-^T \xi = 0, \tag{7}$$

where $\mathbf{1}_+$ and $\mathbf{1}_-$ are vectors filled with entries 1 of the respective dimension of entries and exits.

The third condition of technical feasibility of some joint nomination vector (b, ξ) can be characterized by the existence of vectors q of flows along the edges of the network and π of pressure squares at the nodes satisfying the conditions

$$\mathcal{A}q = \begin{pmatrix} b \\ \xi \end{pmatrix};\ \mathcal{A}^T\pi = -\Phi q\,|q|\,;\ \pi \in [\pi_*, \pi^*]\,. \tag{8}$$

Here, $\mathcal{A}$ is the incidence matrix of the network graph, $\Phi := \mathrm{diag}((\Phi_e))_{e\in E}$ is a diagonal matrix of roughness coefficients and the modulus sign for a vector has to be understood componentwise. The first two equations in (8) correspond to the first two Kirchhoff's Laws (mass conservation and pressure drop), whereas the interval condition imposes bounds on the pressure. It is actually these bounds that constrain the feasibility of nominations b, ξ, see. e.g. [20].

It is the network owners' responsibility to make sure - without knowledge of concrete bilateral delivery contracts between entries and exits - that condition 3. is satisfied for all nominations fulfilling conditions 1. and 2. This requirement clearly imposes a constraint on the booked capacities C_+, C_- via (6) saying for all (b, ξ) satisfying (6), (7) there exists (q, π) satisfying (8). It can be formally written as:

$$\forall\,(b,\xi) : (6)\,,(7)\ \ \exists\,(q,\pi) : (8)\,. \tag{9}$$

Satisfying (9) in a rigorous way would yield (too) small booking capacities at the nodes of the network. Here, the network owner can benefit from the fact that nominations at the exits (gas withdrawn for consumption) are endowed with a typically large historical data basis so that they can be modeled as random vectors obeying some appropriate multivariate distribution. This offers the possibility to relax the 'for all' condition on ξ in a probabilistic sense as to satisfy (9) with sufficiently high probability p. In this way, by choosing p close to one, it is possible to keep a robust satisfaction of technical feasibility while allowing for considerably larger booked capacities. A similar probabilistic modeling of entry nominations would not be justified (although historical data might be available here too) because their outcome is market driven and thus not a genuine random vector.

This motivates the network owner to relax the worst case condition in a probabilistic sense on the side of exits but keeping it on the side of entries. He then arrives at the following probabilistic formulation of feasible booked capacities C_+, C_-:

$$\mathbb{P}\left(\xi \in [0, C_-]\,,\ \forall b \in [-C_+, 0] : \mathbf{1}_+^T b + \mathbf{1}_-^T \xi = 0\ \exists\,(q,\pi) : (8)\right) \geq p. \tag{10}$$

Here, $\mathbb{P}$ refers to a probability measure related with the random vector ξ and $p \in (0,1]$ is a desired probability level chosen by the network owner. The expression on the left-hand side of this inequality provides the probability that a random exit nomination (within booked capacity) combined with an arbitrary entry nomination (within booked capacity and in balance with the exit nomination) is technically feasible.

Now, for a given capacity vector (C_+, C_-) it may turn out that the associated probability on the left-hand side of (10) is larger than the desired minimum probability p, e.g. 0.96 vs. 0.9. This would give the network owner the opportunity to offer larger capacities while still keeping the desired probability p. Therefore, he might be led to determine the largest possible additional capacities (x_+, x_-) he could offer for booking by new clients. This would lead to the following optimization problem:

$$\begin{aligned} &\max w_+^T x_+ + w_-^T x_- \\ &\mathbb{P}\big(\xi \in [0, C_-]\ \ \forall y \in [0, x_-],\ \forall b \in [-C_+ - x_+, 0] : \mathbf{1}_+^T b + \mathbf{1}_-^T \xi + \mathbf{1}_-^T y = 0 \\ &\exists\,(q,\pi) : \mathcal{A}q = \begin{pmatrix} b \\ \xi + y \end{pmatrix};\ \mathcal{A}^T\pi = -\Phi q\,|q|\,;\ \pi \in [\pi_*, \pi^*]\big) \geq p \qquad . \end{aligned} \tag{11}$$

Here, the weight vector w in the objective reflects some preferences the network owner could have in order to offer new booking capacities at different nodes. In the absence of preferences, he could simply choose $w := \mathbf{1}$. Note, that the nomination vector at exits has been split into ξ and y, where ξ refers to the nominations of already existing clients (thus endowed with historical data and amenable to stochastic modeling) while y refers to nominations of potentially new clients without nomination history. As these can therefore not be treated stochastically, they are considered with a 'for all' requirement similar to entry nominations. No such splitting is necessary on the side of entries because nominations have to be considered there with a 'for all' requirement anyway as they cannot be modeled stochastically in a straightforward manner. In the following section, we shall address in detail the capacity maximization problem for exits only, a restriction which allows us numerically to solve the arising entire optimization problem subject to probust constraints. In contrast, Section 4 will focus on entries only and discuss essential issues related with the solution of this alternatively restricted optimization problem.

3 Maximization of booked capacities for exits in a stationary gas network

As mentioned in the introduction, the overall problem of capacity maximization (11) is too complex to be dealt with here. Therefore, we shall focus in a first step on maximizing capacities at exits.

3.1 The capacity maximization problem for several exits and one entry

In the following we will make the assumption that the network is a tree and that there exists only one entry point serving m exits (for an example see Fig 1 below). The presence of cycles in the network

would significantly complicate the numerical solution of the problem. Nonetheless, in Section 3.4, we sketch a possible methodology in the presence of cycles. The restriction to a single entry is made here, in order not to deal with the robust uncertainty related with the splitting of nominations within several entry nodes (see '$\forall b \in$...' condition in (11)) which will be considered later in Section 4 separately. Without loss of generality, we define the entry to be the root of the network labeled by index '0'. For simplicity, we assume moreover that, the booked capacity C_+ of the entry is large enough to meet the maximum possible load by all exits as well as possible extensions thereof after adding additional capacity at the exits as a result of an optimization problem. As a consequence of this constellation our general capacity maximization problem (11) reduces to an exit capacity maximization problem of the form

$$\begin{gathered} \max w_-^T x_- \\ \mathbb{P}\big(\xi \in [0, C_-] \;\; \forall y \in [0, x_-] \; \exists\, (q, \pi) : \\ \mathcal{A}q = \begin{pmatrix} -\mathbf{1}_-^T \xi - \mathbf{1}_-^T y \\ \xi + y \end{pmatrix};\; \mathcal{A}^T \pi = -\Phi q\,|q|\,;\; \pi \in [\pi_*, \pi^*]\,\big) \geq p \quad . \end{gathered} \tag{12}$$

Here, the remaining decision variables are just the extensions of exit capacities. Since no capacity extension for the single entry is intended and since its existing capacity is not constraining by our assumption, the corresponding constraint disappears as well as the balance equation which is just substituted in the description of technical feasibility. The resulting optimization problem does no longer contain entry nominations at all but only random exit nominations ξ and deterministic exit nominations y of new clients along with the additionally allocated booking capacities x_-.

Clearly, the probabilistic constraint in (12) is not yet in the explicit form of the probust constraint (4). This can be achieved in our case thanks to the network being a tree having the single entry as its root. By directing all edges in E away from the root, according to [10], a vector z of exit loads in this configuration is technically feasible, if and only if in the notation introduced above, the inequality system

$$g_{k,l}(z) := h_k(z) + \pi_k^* - h_l(z) - \pi_{*,l} \geq 0 \quad (k, l = 0, \ldots, m) \tag{13}$$

is satisfied, where

$$h_k(z) := \begin{cases} \displaystyle\sum_{e \in \Pi(k)} \Phi_e \left(\sum_{t \succeq H(e)} z_t \right)^2 & \text{if } k \geq 1 \\ 0 & \text{if } k = 0 \end{cases} \quad . \tag{14}$$

In order to explain the definition of functions h_k above, we denote $k \succeq l$ for $k, l \in V$ if the unique directed path from the root to k, denoted $\Pi(k)$, passes through l. $H(e)$ refers to the head of the (directed) arc $e \in E$.

With these specifications, which are fully explicit in terms of the initial data of the problem, we reformulate problem (12) with the aid of inequalities (13) as

$$\begin{gathered} \max w_-^T x_- \\ \mathbb{P}\left(\xi \in [0, C_-] \;\; g_{k,l}\left(\xi + y\right) \geq 0 \quad \forall y \in [0, x_-]\,; \quad \forall k, l = 0, \ldots, m\right) \geq p \end{gathered} \tag{15}$$

is satisfied with that x. The meaning of this constraint is as follows: The capacity extension x_- is feasible if and only if with probability larger than $p \in (0, 1]$ the sum $\xi + y$ of the original random nomination vector and of a new nomination vector can be technically realized for every such new nomination vector in the limits $[0, x_-]$. Clearly, the probust constraint (15) is of the form (5), with $u := y, x := x_-$ and the uncertainty set $\mathcal{U}(x) := [0, x]$.

In [18] it is shown, that the infinite random inequality system

$$g_{k,l}\left(\xi + y\right) \geq 0 \quad \forall y \in [0, x]\,; \quad \forall k, l = 0, \ldots, m$$

inside (15) can be reduced - using (13) and (14) - to the following finite one

$$\sum_{e \in \Pi(k) \setminus \Pi(l)} \Phi_e \left(\sum_{t \succeq H(e)} \xi_t \right)^2 - \sum_{e \in \Pi(l) \setminus \Pi(k)} \Phi_e \left(\sum_{t \succeq H(e)} \xi_t + (x_-)_t \right)^2 \geq \pi_{*,l} - \pi_k^*; \quad \forall k, l = 0, \ldots, m \tag{16}$$

For the random vector ξ of stochastic exit nominations we will suppose that it follows a truncated multivariate Gaussian distribution:

$$\xi \sim \mathcal{TN}(\mu, \Sigma, [0, C_-]).$$

More precisely, the distribution of ξ is obtained by truncating an m-dimensional Gaussian distribution with mean μ and covariance matrix Σ to an m-dimensional rectangle $[0, C_-]$ representing the (historical) booked capacity at exit node i. By definition of truncation, this means that there exists a Gaussian random vector $\tilde{\xi} \sim \mathcal{N}(\mu, \Sigma)$ such that

$$\mathbb{P}\left(\xi \in A\right) = \frac{\mathbb{P}\left(\tilde{\xi} \in A \cap [0, C_-]\right)}{\mathbb{P}\left(\tilde{\xi} \in [0, C_-]\right)}$$

holds true for all Borel measurable subsets $A \subseteq \mathbb{R}^m$. Hence, in order to determine probabilities under a truncated Gaussian distribution, it is sufficient to be able to determine probabilities under a Gaussian distribution itself. Applying this observation to the probabilistic constraint (15) and combining it with (16) yields the equivalent description

$$\mathbb{P}\big(\tilde{\xi} \in [0, C_-] : \sum_{e \in \Pi(k) \setminus \Pi(l)} \Phi_e \left(\sum_{t \succeq H(e)} \tilde{\xi}_t \right)^2 - \sum_{e \in \Pi(l) \setminus \Pi(k)} \Phi_e \left(\sum_{t \succeq H(e)} \tilde{\xi}_t + (x_-)_t \right)^2 \geq \pi_{*,l} - \pi_k^*; \quad \forall k, l = 0, \ldots, m\big) \geq p \cdot \mathbb{P}\left(\tilde{\xi} \in [0, C_-]\right). \tag{17}$$

This is now, in contrast to (15) a conventional probabilistic constraint over a finite inequality system. In order to deal algorithmically with the probabilistic constraint (17), one has evidently to be able to calculate for each fixed decision vector x_- the probabilities occurring there, as well as their derivatives with respect to x_-. In the following section we briefly sketch the methodology used here.

3.2 Spheric-Radial decomposition of Gaussian random vectors

From the well-known spheric-radial decomposition (see, e.g., [9]) of a Gaussian random vector $\tilde{\xi} \sim \mathcal{N}(\mu, \Sigma)$ it follows that the probability of an arbitrary Borel measurable subset M of $\mathbb{R}^m$ may be represented as the following integral over the unit sphere $\mathbb{S}^{m-1}$:

$$\mathbb{P}\left(\tilde{\xi} \in M\right) = \int\limits_{v \in \mathbb{S}^{m-1}} \mu_\chi\left(E(v)\right) d\mu_\eta(v).$$

Here, μ_χ refers to the one-dimensional Chi-distribution with m degrees of freedom, μ_η is the uniform distribution on $\mathbb{S}^{m-1}$ and

$$E(v) := \{r \geq 0 | \mu + rPv \in M\},$$

where P is a factor from a decomposition $\Sigma = PP^T$ of the covariance matrix Σ. Following these remarks, the probability on the left-hand side of (17) (depending also on the decision variable x_-) can be represented as

$$\int\limits_{v \in \mathbb{S}^{m-1}} \mu_\chi \left(E(v, x_-) \right) d\mu_\eta(v), \tag{18}$$

where

$$E(v, x_-) = \{r \geq 0 | \mu + rPv \in [0, C_-]\} \cap \bigcap_{k,l=0,\ldots,m} E^{k,l}(v, x_-) \tag{19}$$

and, with P_t denoting row number t of P, for $k, l = 0, \ldots, m$:

$$\begin{aligned} E^{k,l}(v, x_-) := \big\{ r \in \mathbb{R} | \\ \sum_{e \in \Pi(k) \setminus \Pi(l)} \Phi_e \left(\sum_{t \succeq H(e)} \mu_t + rP_t v \right)^2 - \sum_{e \in \Pi(l) \setminus \Pi(k)} \Phi_e \left(\sum_{t \succeq H(e)} \mu_t + rP_t v + (x_-)_t \right)^2 \\ \geq \pi_{*,l} - \pi^*_k \big\}. \end{aligned} \tag{20}$$

In order to evaluate the integrand in (18), one has to be able to characterize (for each given $v \in \mathbb{S}^{m-1}$ and $x_- \in \mathbb{R}^m$) the set $E(v, x_-)$ and to determine its Chi probability. The latter task is easily accomplished, whenever the set $E(v, x_-)$ can be represented as a finite union of intervals because there exist numerically highly precise approximations of the one dimensional Chi distribution function.

Hence, we are left with the task of efficiently representing $E(v, x_-)$ as a finite union of intervals. This is easily done for the first set in the intersection providing $E(v, x_-)$ in (19) which can be shown either to be empty or an interval:

$$\begin{aligned} &\big\{ r \geq 0 | \mu + rPv \in [0, C_-] \big\} = \\ &\begin{cases} \emptyset & \text{if } \exists t \in \{1, \ldots, m\} : P_t v = 0,\ \mu_t \notin [0, C_{-,t}] \\ [L, R] & \text{else;} \end{cases} \end{aligned} \tag{21}$$

$$\begin{aligned} L &:= \max \left\{ 0, \max_{P_t v > 0} \frac{-\mu_t}{P_t v}, \max_{P_t v < 0} \frac{C_{-,t} - \mu_t}{P_t v} \right\} \text{ and} \\ R &:= \min \left\{ \min_{P_t v > 0} \frac{C_{-,t} - \mu_t}{P_t v}, \min_{P_t v < 0} \frac{-\mu_t}{P_t v} \right\}. \end{aligned}$$

As for the second part of the intersection in (19), we will provide for each k, l an explicit representation of the set $E^{k,l}(v, x)$ either as a single interval or as the disjoint union of two intervals, such that the union over all these sets (and the first set determined above) is readily obtained in the form of a finite union of disjoint intervals. Indeed, upon developing the expressions in (20) in terms of r, one arrives at the representation

$$E^{k,l}(v, x_-) = \{r \in \mathbb{R} | \alpha^{k,l} r^2 + \beta^{k,l} r + \gamma^{k,l} \geq 0\} \quad (k, l = 0, \ldots, m),$$

where, for $k, l = 0, \dots, m$:

$$\begin{aligned}
\alpha^{k,l} &:= \sum_{e \in \Pi(k) \setminus \Pi(l)} \Phi_e \left(\sum_{t \succeq H(e)} P_t v \right)^2 - \sum_{e \in \Pi(l) \setminus \Pi(k)} \Phi_e \left(\sum_{t \succeq H(e)} P_t v \right)^2 \\
\beta^{k,l} &:= 2 \sum_{e \in \Pi(k) \setminus \Pi(l)} \Phi_e \left(\sum_{t \succeq H(e)} \mu_t \right) \left(\sum_{t \succeq H(e)} P_t v \right) \\
&\quad -2 \sum_{e \in \Pi(l) \setminus \Pi(k)} \Phi_e \left(\sum_{t \succeq H(e)} \mu_t + x_{-,t} \right) \left(\sum_{t \succeq H(e)} P_t v \right) \\
\gamma^{k,l} &:= \sum_{e \in \Pi(k) \setminus \Pi(l)} \Phi_e \left(\sum_{t \succeq H(e)} \mu_t \right)^2 - \sum_{e \in \Pi(l) \setminus \Pi(k)} \Phi_e \left(\sum_{t \succeq H(e)} \mu_t + x_{-,t} \right)^2 \\
&\quad + \left(p_k^{\max}\right)^2 - \left(p_l^{\min}\right)^2 .
\end{aligned}$$

This leads, by case distinction and elementary calculus, to the following explicit representation of $E^{k,l}(v, x_-)$ for $k, l = 0, \dots, m$:

$$E^{k,l}(v, x_-) =$$

$$\begin{cases}
\emptyset & \text{1) or 2)} \\
\mathbb{R} & \text{3) or 4)} \\
\left[-\frac{\gamma^{k,l}}{\beta^{k,l}}, \infty \right) & \text{5)} \\
\left(-\infty, -\frac{\gamma^{k,l}}{\beta^{k,l}} \right] & \text{6)} \\
\left(-\infty, \frac{-\beta^{k,l} - \sqrt{\left(\beta^{k,l}\right)^2 - 4\alpha^{k,l}\gamma^{k,l}}}{2\alpha^{k,l}} \right] \cup \left[\frac{-\beta^{k,l} + \sqrt{\left(\beta^{k,l}\right)^2 - 4\alpha^{k,l}\gamma^{k,l}}}{2\alpha^{k,l}}, \infty \right) & \text{7)} \\
\left[\frac{-\beta^{k,l} + \sqrt{\left(\beta^{k,l}\right)^2 - 4\alpha^{k,l}\gamma^{k,l}}}{2\alpha^{k,l}}, \frac{-\beta^{k,l} - \sqrt{\left(\beta^{k,l}\right)^2 - 4\alpha^{k,l}\gamma^{k,l}}}{2\alpha^{k,l}} \right] & \text{8)}
\end{cases},$$

where the case study is done according to

$$\begin{aligned}
&\text{1)} && \alpha^{k,l} = \beta^{k,l} = 0,\ \gamma^{k,l} < 0, \\
&\text{2)} && \alpha^{k,l} < 0,\ \left(\beta^{k,l}\right)^2 < 4\alpha^{k,l}\gamma^{k,l}, \\
&\text{3)} && \alpha^{k,l} = \beta^{k,l} = 0,\ \gamma^{k,l} \geq 0, \\
&\text{4)} && \alpha^{k,l} > 0,\ \left(\beta^{k,l}\right)^2 < 4\alpha^{k,l}\gamma^{k,l}, \\
&\text{5)} && \alpha^{k,l} = 0,\ \beta^{k,l} > 0, \\
&\text{6)} && \alpha^{k,l} = 0,\ \beta^{k,l} < 0, \\
&\text{7)} && \alpha^{k,l} > 0,\ \left(\beta^{k,l}\right)^2 \geq 4\alpha^{k,l}\gamma^{k,l}, \\
&\text{8)} && \alpha^{k,l} < 0,\ \left(\beta^{k,l}\right)^2 \geq 4\alpha^{k,l}\gamma^{k,l}.
\end{aligned}$$

Along with (21) we may use this explicit description in order to efficiently represent the set $E(v, x_-)$ in (19) as the desired finite union of intervals by determining the finite intersection of sets which are intervals or disjoint unions of intervals.

It is important to note that, at the same time, the partial derivatives of the probability with respect to the decision variable x_- can be calculated as a spherical integral of type (18) again, however with a different integrand which is easily obtained from the partial derivatives of the initial data [2]. In these gradient formula, the same disjoint union of intervals as in the computation of the probability itself is employed. The spherical integrals can be approximated by finite sums using Quasi-Monte Carlo sampling on the sphere (see, e.g., [5]). Then, for each sampled direction v on the sphere, one may update first the probability itself and then, simultaneously, the gradient of the probability with respect to x_- by using the same disjoint union of intervals in both cases. This approach makes the gradient come almost for free as far as computation time is concerned. Having access to values and gradients of the probabilistic constraint (17), one may set up an appropriate nonlinear optimization solver for solving (15). For the subsequent numerical results, we employed a simple projected gradient method.

3.3 Numerical results for an example

As an illustrating example we considered a network as displayed in Fig. 1 with one entry (filled black circle) and 26 exits. The parameters of the network (i.e., pressure bounds, roughness coefficients, truncated Gaussian distribution for the random nominations at exits) were chosen in realistic quantities that are modified versions from real data.

We didn't assume any preferences in the allocation of new capacities, hence the weight vector in the objective of (15) was chosen as $w_- := \mathbf{1}_-$. The colored rings around exit points refer to the optimal cumulative capacities (historical+new), i.e. $C_- + x_-$ after maximization, upon choosing probability levels $p = 0.95, 0.9, 0.85, 0.8$. It can be clearly seen, how decreasing of the probability level allows for increasing the allocation of capacity in certain regions of the network.

Fig. 2 illustrates how the computed solution for a probability level $p = 0.8$ works for two random exit nomination scenarios ξ simulated a posteriori according to the chosen truncated multivariate Gaussian distribution. The first scenario is feasible because one could uniformly add a common capacity to every exit (green color) in order to satisfy this scenario. In contrast, the second scenario is infeasible because one would have to (uniformly) reduce the capacities by an amount corresponding to the dark red rings, in order to satisfy this scenario. When simulating a large set of such scenarios, say 1000, it would turn out that according to the probability level $p = 0.8$ approximately 800 are feasible, while 200 are infeasible.

3.4 Methodology in the presence of cycles

It is generally acknowledged that the presence of cycles in gas networks is both realistic for applications and demanding for formal analysis. In what follows we elucidate this at calculating the probability of feasible nominations in a gas network with cycles.

Networks with a single or with multiple node-disjoint cycles are covered in [10] which essentially relies on the explicit formula for the roots of univariate real polynomials which is part of basic calculus.

If cycles in a gas network are sharing edges, then the approach via the mentioned formula is no longer valid. It also cannot be stretched to more general cases. A first alternative attempt in this respect has been undertaken recently in [11] for networks with up to three mutually interconnected cycles.

To display the state-of-the-art in calculating by spheric-radial decomposition probabilities of sets of

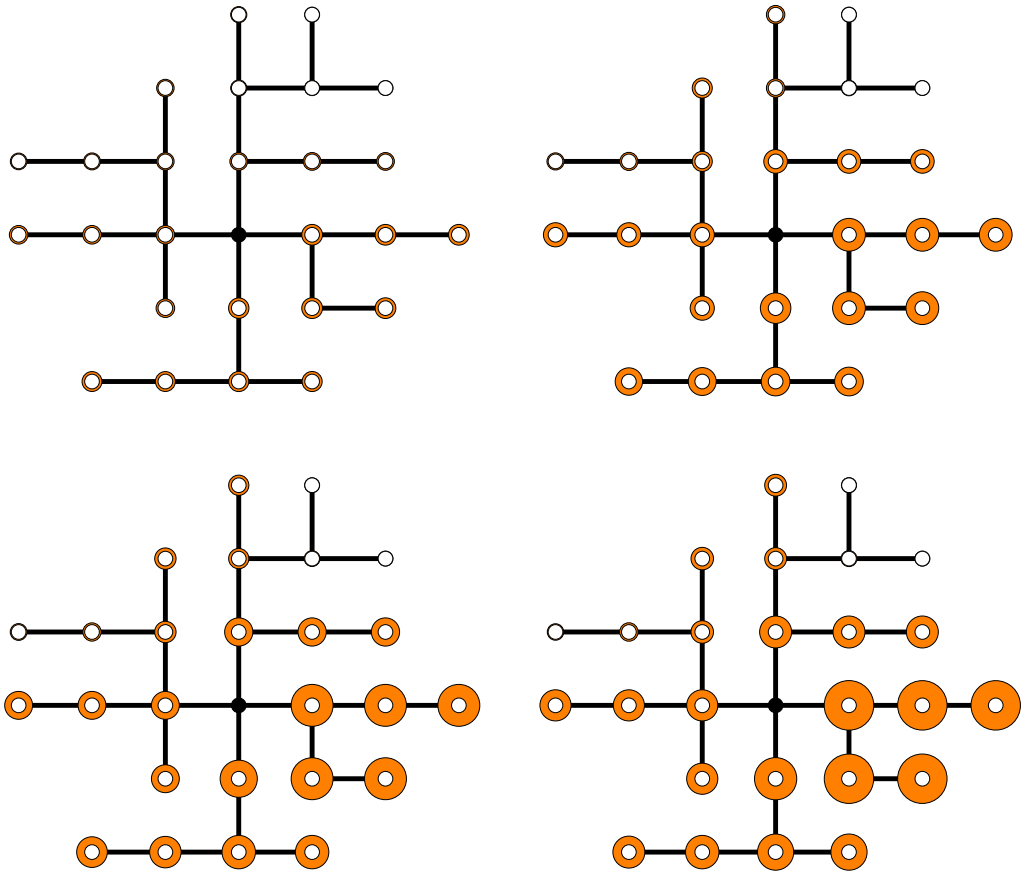

Figure 1: Solution of the capacity maximization problem at exits for different probability levels: 0.95 (top left); 0.9 (top right); 0.85 (bottom left); 0.8 (bottom right).

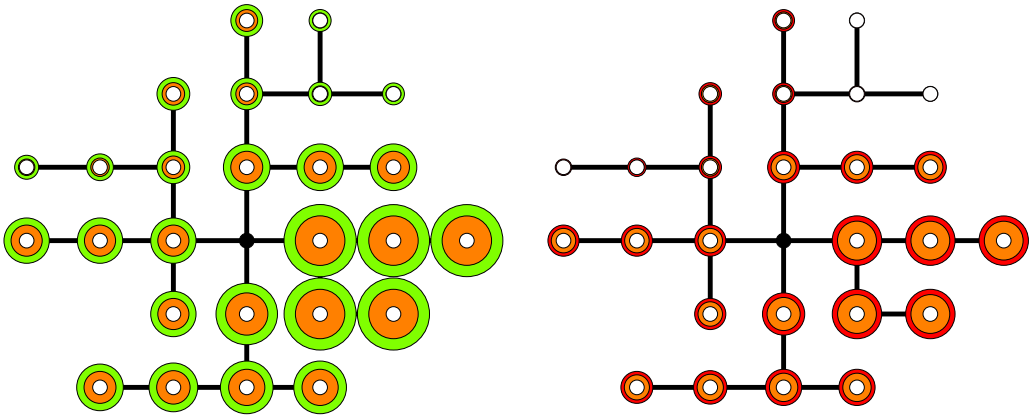

Figure 2: Two scenarios for random exit loads ξ according to the chosen multivariate truncated Gaussian distribution. Left: feasible scenario; Right: infeasible scenario.

feasible nominations in gas networks with cycles, consider again

$$E_i := E(v_i) = \{r \geq 0 \,|\, \mu + rPv_i \in M\}$$

for every sample $v_1, ..., v_s$ on the sphere. Since the set E_i can be expressed as a finite union of disjoint intervals, $E_i = \cup_{j=1}^{l}[a_j, b_j]$, for calculating its probability, it is sufficient to determine all points where the ray $rPv_i + \mu$ enters or exits the set of feasible load vectors M.

With cycles, the matrix $\mathcal{A}$ decomposes into a basis part $\mathcal{A}_B$ and a non-vacuous non-basis part $\mathcal{A}_N$ whose columns correspond to the fundamental cycles with respect to the tree behind $\mathcal{A}_B$. Accordingly q, Φ are split into q_B, q_N and Φ_B, Φ_N.

In [10] it is shown that a given load $(-\mathbf{1}^\top\xi, \xi)$ is feasible iff there exists a q_N such that

$$\begin{aligned}
\mathcal{A}_N^\top g(\xi, q_N) &= \Phi_N|q_N|q_N && (22)\\
\min_{i=1,\dots,|V|-1}[\pi_i^* + g_i(\xi, q_N)] &\geq \max_{i=1,\dots,|V|-1}[\pi_{*,i} + g_i(\xi, q_N)] && (23)\\
\pi_{*,0} &\leq \min_{i=1,\dots,|V|-1}[\pi_i^* + g_i(\xi, q_N)] && (24)\\
\pi_0^* &\geq \max_{i=1,\dots,|V|-1}[\pi_{*,i} + g_i(\xi, q_N)] && (25)
\end{aligned}$$

with

$$g : \mathbb{R}^{|V|-1} \times \mathbb{R}^{|N|} \to \mathbb{R}^{|V|-1}, \quad g(s,t) := \left(\mathcal{A}_B^\top\right)^{-1}\Phi_B\left|\mathcal{A}_B^{-1}(s - \mathcal{A}_N t)\right|\left(\mathcal{A}_B^{-1}(s - \mathcal{A}_N t)\right).$$

Having in mind spheric-radial decomposition and the sets E_i, insert $\xi(r) = rPv_i + \mu$ into the above characterization of feasible loads and dissolve the min, max expressions. Then E_i consists of all $r \in \mathbb{R}_{\geq 0}$ for which there is a q_N such that

$$\begin{aligned}
\mathcal{A}_N^\top g(rPv_i + \mu, q_N) &= \Phi_N|q_N|q_N && (26)\\
\pi_j^* + g_j(rPv_i + \mu, q_N) &\geq \pi_{*,k} + g_k(rPv_i + \mu, q_N) \\
&\quad \text{for all } j,k = 1,\dots,|V|-1, \;\; j \neq k && (27)\\
\pi_{*,0} &\leq \pi_j^* + g_j(rPv_i + \mu, q_N) \\
&\quad \text{for all } j = 1,\dots,|V|-1 && (28)\\
\pi_0^* &\geq \pi_{*,j} + g_j(rPv_i + \mu, q_N) \\
&\quad \text{for all } j = 1,\dots,|V|-1 && (29)
\end{aligned}$$

To decide, for a given sample point v_i, whether the ray $rPv_i + \mu$ enters or exits the set of feasible load vectors M and, in the affirmative, compute an entry or exit point, the following basic procedure is possible: Augment one of the inequalities of the system (27)-(29) as an equation to (26) yielding a system of $|N| + 1$ degree-2 multivariate polynomial equations with $|N| + 1$ unknowns.

Notice that the above considerations hold for gas networks with arbitrary cardinality $|N|$ of non-basis columns in $\mathcal{A}$ which is the reason for displaying the material here. Of course, the number of augmentations, and hence the number of passes through some polynomial-equation solver can become exorbitant.

A first attempt on the latter via computer algebra is reported in [11] for $|N| \leq 3$. In the core of the method there are Gröbner bases inducing "triangular" representations of the polynomial equations, allowing for "reverse propagation" of solutions, in the spirit of Gaussian elimination, with multivariate quadratic polynomials instead of linear forms.

In contrast with gradient-type analytical solvers, algebraic solvers using symbolic computation usually detect infeasibility of the system under consideration much faster. These methods rely on iterating bases of ideals. Emptiness follows as soon as there arises a constant polynomial in the current ideal basis.

There are a number of possible improvements, some of which investigated in [11] that deserve further explorations: identifying and removing redundant inequalities in (27)-(29), studying the special structure of the system (26) and exploring the impact of "Comprehensive Gröbner Systems" that were developed for parametric polynomial equations, see [22].

4 Capacity maximization under uncertain loads and uncertain distribution of entry nominations

After discussing the methodology for the case of uncertain exit loads, we address the case of uncertain entry loads. Instead of solving the full capacity problem, we focus on the probust constraint of Problem (11). In the following, we present an algorithm that approximates the probability in the probust constraint (10). To solve the capacity problem, we subsequently embed this algorithm within a gradient free pattern search algorithm.

Analogously to Section 3, the spheric radial decomposition is applied. Let m be the number of exit nodes, $v \in \mathbb{S}^{m-1}$ be a sampled vector, $\mu \in \mathbb{R}^m$ be the mean and P is obtained from the covariance matrix of the Gaussian distribution of the exit loads. As discussed in Section 3.2, we need to determine the length of the intersection of the rays $\mu + rPv$ with the set of robust feasible exit loads M, i.e. the set

$$E(v) := \{r \in \mathbb{R}_{\geq 0} \mid \mu + rPv \in M\}.$$

As discussed in Section (3.2), this results in a finite union of disjoint intervals $E(v) = \cup_{j=0}^{t} E_j(v)$. The Chi probability of $E(v)$ can be bounded from below by $E_k(v)$ for $k = 0, \ldots, t$. In particular, we bound the length of the first interval $E_0(v)$, i.e. the interval with minimum 0, from below by applying a problem specific binary search which in every iteration decides whether a given number is an element of $E_0(v)$. In theory, this decision is made by solving a nonlinear optimization problem (NLP) which checks whether all pressures lie within prescribed bounds for a given realization of (squared) pressure and flow values. In order to make sure that all potential violations of pressure bounds are detected, globally optimal solutions are required. In order to achieve this, we linearize the NLPs. As binary variables are introduced for the piecewise relaxation, a Mixed-Integer Linear Problem (MIP) is solved instead of the original NLP. The resulting MIP can be solved globally with off-the-shelf-software.

In the remainder of this section, we present the developed algorithm that yields lower bounds on the length of $E_0(v)$. We prove its correctness under the assumption that there exists a node with fixed pressure. This is not a critical assumption in reality, since gas is injected at some entry node and we can assume that the pressure at this node is known.

In the following, we call a set S star-shaped with respect to s^* if for all $\lambda \in [0, 1]$ and for all $s \in S$ the convex combination $\lambda s + (1 - \lambda)s^* \in S$. We note that if the set of robust feasible exit loads is star-shaped with respect to μ, the whole set $E(v)$ is an interval. Our approach is particularly effective in this case, since this implies $E_0(v) = E(v)$. However, since we can also carry out the analysis in general, we do not limit ourselves to star-shaped sets.

We conclude this section by the presentation of computational results that show the effectiveness of the method.

4.1 Methodology for general stationary networks

Analogously to Section 3, we assume that the capacities at the exits are large enough to meet the maximum possible loads by all entries. As introduced in Section 2, we assume that the exit loads follow a Gaussian distribution, as enough historical data are available. In contrast, for the entry loads, the outcome of the entry nominations is market driven which means that we cannot rely on a method that is purely probabilistic, see Section 1. Instead, we will develop a probust approach. Furthermore, instead of solving optimization problem (11), we solve the following decision problem: For a given exit load ξ, we have to ensure the feasibility of every possible entry load b with a probability of at least p. Since we have to take extensions x_+ of the entry capacities C_+ into account, the possible entry nominations, i.e., the uncertainty set, is

$$\mathcal{U}(\xi, x_+) := \{b \in [-C_+ - x_+, 0] : \mathbf{1}_+^T b + \mathbf{1}_-^T \xi = 0\}. \tag{30}$$

The probust constraint of problem (11) is then

$$\mathbb{P}\left(\xi \geq 0 : \ \forall b \in \mathcal{U}(\xi, x_+)\ \exists (q, \pi) : \ Aq = \begin{pmatrix} b \\ \xi \end{pmatrix},\ A^T \pi = -\Phi |q| q\right) \geq p. \tag{31}$$

We introduce the following definition:

Definition 1. *Let an exit nomination $\xi \geq 0$ and a capacity extension $x_+ \geq 0$ be given. If for every $b \in \mathcal{U}(\xi, x_+)$ there exists a flow q and a pressure π, such that* (8) *is satisfied, (ξ, x_+) is called* robust feasible*.*

In other words, in the probust constraint (31), we want for $\xi \geq 0$ and for $x_+ \geq 0$ to ensure robust feasibility of x_+ with a probability of at least p.

As $\mathcal{U}(\xi, x_+)$ contains in general infinitely many points, answering robust feasibility for (ξ, x_+) requires the solution of a semiinfinite feasibility problem already for fixed x_+. As this is already a challenge on its own, we decide whether (ξ, x_+) is feasible for problem (11), i.e. we check whether constraint (31) is satisfied. This decision problem is denoted by DecProb(ξ, x_+).

In order to answer DecProb(ξ, x_+), we develop an optimization problem and apply the spheric radial decomposition analogously to Section 3.2. Let $v \in \mathbb{S}^{m-1}$, a capacity extension $x_+ \geq 0$ and $r \geq 0$ be given. Instead of analyzing the entire uncertainty set (30), we analyze the rays which arise in the spheric radial decomposition. Hence set (30) is additionally parametrized by v and r and substituted by

$$\mathcal{U}(r, v, x_+) := \{b \in [-C_+ - x_+, 0] : \mathbf{1}_+^T b + \mathbf{1}_-^T (\mu + rPv) = 0\}. \tag{32}$$

It has been discussed in Section 3.2 that validating (31) for each ray $\mu + rPv$ amounts to computing

$$\begin{aligned} E(v, x_+) := \{r \geq 0 : \forall b \in \mathcal{U}(r, v, x_+)\ \exists (\pi, q) : \\ Aq = \begin{pmatrix} b \\ \mu + rPv \end{pmatrix},\ A^T \pi = -\Phi |q| q\}, \end{aligned}$$

which contains all nonnegative r for which all entry nominations of the uncertainty set $\mathcal{U}(r, v, x_+)$ are realizable. As explained in Section 3.2, we can write $E(v, x_+) = \bigcup_{j=0}^{t} E_j(v, x_+)$ as a finite union of

disjoint intervals. In the following, we only take the first interval $E_0(v, x_+)$ with minimum 0 into account; $|E_0(v, x_+)|$ denotes the length of $E_0(v, x_+)$. The Chi probability of $E_0(v, x_+)$ is a lower bound of the Chi probability of $E(v, x_+)$ which, consequently, results in a lower bound for the probability in (31). Hence our goal is to bound $|E_0(v, x_+)|$ from below.

To this end, we exploit that DecProb($\mu + rPv, x_+$) is always answered positively for a gas network if the pressure is unbounded at all nodes ([20], Theorem 7.1). The respective solutions (π, q) are labeled *pressure flow solutions*. As in real gas network operations the pressures are bounded, we introduce so-called *penalty functions* for every $u \in V$, in formulas,

$$f_u \colon \mathbb{R} \to \mathbb{R}^+,\ \pi_u \mapsto \max\{0, \pi_{*,u} - \pi_u, \pi_u - \pi_u^*\}.$$

If $f_u(\pi_u) > 0$ for a node $u \in V$, π_u lies outside its bounds. Consequently, $\pi \in [\pi_*, \pi^*]$ if and only if

$$\sum_{u \in V} f_u(\pi_u) = 0. \tag{33}$$

Thus, to decide whether (33) is true for some (π, q) we introduce the optimization problem

$$\begin{aligned} \max & \sum_{u \in V} f_u(\pi_u), \\ \text{s.t.} \quad & Aq = \begin{pmatrix} b \\ \mu + rPv \end{pmatrix}, \\ & A^T \pi = -\Phi |q| q, \\ & \mathbf{1}_-^T(\mu + rPv) + \mathbf{1}_+^T b = 0, \\ & b \in [-C_+ - x_+, 0], \\ & 0 \le r \le R. \end{aligned} \tag{Pen(R, v, x_+))}$$

If we assume that the pressure at one node is fixed, we will show in the following theorem that $R \in E_0(v, x_+)$ and hence $[0, R] \subset E_0(v, x_+)$ if and only if the optimal value of problem (Pen(R, v, x_+)) is zero.

Theorem 1. *Let $v \in \mathbb{S}^{m-1}$ and let $x^+ \ge 0$ be a capacity extension at the entries. Assume that the pressure at one node is fixed. Then $R \in E_0(v, x_+)$ if and only if problem* (Pen(R, v, x_+)) *is solvable with optimal value 0.*

Proof. Since $f_u(\pi_u)$ is nonnegative for all nodes $u \in V$, the optimal value of (Pen(R, v, x_+)) is at least zero.

Assume on the one hand that $R \in E_0$. Hence, for an arbitrary choice of $r \in [0, R]$ and for any entry nomination $b \in \mathcal{U}(r, v, x_+)$, there exist a flow vector q and a squared pressure vector π such that the nomination $(b, \mu + rPv)$ is feasible. Consequently, $\pi \in [\pi_*, \pi^*]$ and the objective value for (r, b, π, q) is 0. Due to the fact that the pressure is fixed at one node, the pressure flow solution is unique, see Theorem 7.2. in [20]. Hence the objective value is zero for all feasible solutions of (Pen(R, v, x_+)).

On the other hand, assume that the optimal value is zero. Therefore, for all $b \in \mathcal{U}(r, v, x_+)$ there exist a flow q and a squared pressure π, such that (r, b, π, q) is feasible for (Pen(R, v, x_+)). Since the optimal value is zero, $\pi \in [\pi_*, \pi^*]$. Hence the pressures lie within their prescribed bounds and $R \in E_0(v, x_+)$. Thus, the proof is finished. □

We note that the assumption of a fixed pressure is crucial in the proof of Theorem 1. Unless this assumption is satisfied, the pressure values are not necessarily unique and problem (Pen(R, v, x_+)) can be unbounded although $R \in E_0(v, x_+)$.

Problem (Pen(R, v, x_+)) can be used to decide whether $R \in E_0(v, x_+)$. Since $E_0(v, x_+)$ is an interval, we can approximate its length using a standard binary search which solves the subproblem (Pen(R, v, x_+)) in every iteration.

A binary search algorithm starts with a lower and an upper bound. Since $0 \in E(v, x_+) \subset \mathbb{R}_{\geq 0}$, we choose zero as a lower bound. A trivial upper bound for $E(v, x_+)$ is given by the exit capacities

$$0 \leq \mu + rPv \leq C_-.$$

A tighter bound is given as follows. Due to (8), the pressure drop constraint

$$\pi_i - \pi_j = \Phi_{i,j} \, |q_{i,j}| \, q_{i,j} \tag{34}$$

holds for every arc $(i, j) \in E$. Since the right hand side of (34) is invertible and the pressures are bounded, we can derive flow bounds for every arc which do not depend on the actual nomination. In the following, these flow bounds, which are called *implicit flow bounds* and are denoted by q_* and q^*, are exploited to determine an improved upper bound for $E(v, x_+)$:

Lemma 1. *Let $v \in \mathbb{S}^{m-1}$, let q_* and q^* be the implicit flow bounds and $x_+ \geq 0$ be a capacity extension at the entry nodes. For a node $u \in V$, let $\delta^-(u)$ denote the set of incoming arcs and let $\delta^+(u)$ denote the set of outgoing arcs. Then an upper bound for $E(v, x_+)$ is given by the optimal value of the optimization problem*

$$\begin{aligned}
&\max r, \\
&\textit{s.t.} \quad 0 \leq \mu + rPv \leq C_-, \\
&\qquad \sum_{e \in \delta^-(u)} q_e^* - \sum_{e \in \delta^+(u)} q_{*,e} \geq \mu_u + r(Pv)_u \; \forall u \in V_-, \\
&\qquad \sum_{e \in \delta^-(u)} q_{*,e} - \sum_{e \in \delta^+(u)} q_e^* \leq \mu_u + r(Pv)_u \; \forall u \in V_-, \\
&\qquad r \geq 0.
\end{aligned} \tag{UB(v, x_+)}$$

Proof. Since we are interested in an upper bound for $E(v, x_+)$, $0 \leq \mu + rPv \leq C_-$ and $r \geq 0$ are satisfied. Furthermore, Kirchoff's first law demands

$$\sum_{e \in \delta^-(u)} q_e - \sum_{e \in \delta^+(u)} q_e = \mu_u + r(Pv)_u \quad \forall u \in V_-$$

for a flow q. Substituting the flow variables by the implicit flow bounds q_* and q^* results in

$$\sum_{e \in \delta^-(u)} q_e^* - \sum_{e \in \delta^+(u)} q_{*,e} \geq \mu_u + r(Pv)_u \quad \forall u \in V_-$$

and

$$\sum_{e \in \delta^-(u)} q_{*,e} - \sum_{e \in \delta^+(u)} q_e^* \leq \mu_u + r(Pv)_u \quad \forall u \in V_-.$$

This concludes the proof. □

Denote the optimal value of problem (UB(v, x_+)) as z, hence $|E_0(v, x_+)| \in [0, z]$. Algorithm 1 summarizes the procedure for bounding $|E_0(v, x_+)|$ from below. In every iteration of Algorithm 1, (Pen(R, v, x_+)) is solved for a given R. With a given tolerance tol, Algorithm 1 bounds $|E_0(v, x_+)|$ from below with an error of at most tol. Due to Theorem 1 and Lemma 1, Algorithm 1 terminates with a correct lower bound. Since the algorithm applies binary search with start interval $[0, z]$, its number of iterations is $\lfloor \log_2(\frac{z}{\mathrm{tol}}) \rfloor$.

Algorithm 1 Finding a lower bound for $|E_0(v, x_+)|$ through Bisection

Input: Sphere vector $v \in \mathbb{S}^{m-1}$, capacity $x_+ \geq 0$, tolerance $\mathrm{tol} > 0$
Output: $R \in \mathbb{R}$, such that $|E_0(v, x_+)| - R < \mathrm{tol}$

```
l ← 0
z ← Optimal value of (UB(v, x_+))
while |z − l| > tol do
    R ← (z+l)/2
    Solve (Pen(R, v, x_+))
    if (Pen(R, v, x_+)) is infeasible then
        z ← R
    else
        let z* be the optimal value of (Pen(R, v, x_+))
        if z* = 0 then
            l ← R
        else
            z ← R
        end if
    end if
end while
R ← l
return R
```

In every iteration of Algorithm 1, l denotes a lower bound for $|E_0(v, x_+)|$. Therefore, the lower bound for the variable r in (Pen(R, v, x_+)) is set to l, since we do not have to check whether $R \in E_0(v, x_+)$ twice.

In practice, Algorithm 1 is applied for every vector v that is sampled in the spheric radial decomposition. Afterwards, the lower bounds for $|E_0(v, x_+)|$ for every v are used to check the validity of (31). However, (Pen(R, v, x_+)) is a NLP that has to be solved to global optimality. In order to circumvent this problem in practice, we aim to relax the nonlinear pressure drop constraint (34) for every $(i, j) \in E$. The applied procedure has been developed in [8]. For the relaxation, linear splines are used to interpolate $\Phi_{i,j}|q_{i,j}|q_{i,j}$. For a given *linearization error* $\epsilon > 0$, the linear splines $s_{i,j}(q_{i,j})$ are constructed such that

$$s_{i,j}(q_{i,j}) - \epsilon \leq \Phi_{i,j}|q_{i,j}|q_{i,j} \leq s_{i,j}(q_{i,j}) + \epsilon \tag{35}$$

for every $(i, j) \in E$. Therefore, we substitute (34) with

$$s_{i,j}(q_{i,j}) - \epsilon \leq \pi_i - \pi_j \leq s_{i,j}(q_{i,j}) + \epsilon \tag{36}$$

for all $(i, j) \in E$. The splines $s_{i,j}(q_{i,j})$ are modeled with the incremental method, see [23]. Hence, subproblem (Pen(R, v, x_+)) is relaxed to a MIP which can be solved to global optimality. It has been

shown that this approach leads to a very effective method for gas network optimization problems that is able to solve very large instances in practice, see [20].

For applying the incremental method, we require bounds for the flow variables $q_{i,j}$. However, we cannot use the implicit flow bounds q_* and q^* since the pressure is not bounded in (Pen(R, v, x_+)). Instead, we apply the preprocessing developed in [3] where the pressure bounds are neglected as well. Since the pressure bounds are treated as penalty terms in Problem (Pen(R, v, x_+)), the derived flow bounds are valid for the incremental method, i.e. the set of solutions is not altered. Furthermore, due to (35) and (36), the optimal value of the linearized problem is an upper bound for the optimal value of the original problem. Therefore, if the optimal value of the linearized problem is zero, the optimal value of Problem (Pen(R, v, x_+)) is zero as well. Due to Theorem 1 it follows that $R \in E_0(v, x_+)$. This implies the robust feasibility of $(\mu + RPv, x_+)$. Since this applies for all $R \geq 0$ and for all $v \in \mathbb{S}^{m-1}$, constraint (31) is satisfied if the derived lower bound is larger than the desired probability level p.

This concludes the presentation of the developed algorithm which is applicable for general gas networks. Note that the result of our algorithm is a lower bound for the probability for two reasons: On the one hand, approximation errors are caused by the binary search and the MIP linearization. However, we can limit the influence of those by reducing tol and ϵ in Algorithm (1) and the inequalities (35), respectively. On the other hand, we approximate $|E_0(v, x_+)|$ which is in general not equal to $|E(v, x_+)|$. However, as already mentioned at the beginning of the section, in the case of star-shaped robust feasible exit loads, $E(v, x_+) = E_0(v, x_+)$ is an interval and the entire ray is calculated.
In the next subsection, we evaluate Algorithm 1 with respect to quality of the obtained solutions and running time.

4.2 Numerical results

We modify the gas network instance of Section 3.2 by adding a second entry next to the first entry (black filled node). In addition, we fix the pressure at a leaf node. Beyond that, we provide sphere vectors v by sampling a collection of 10 000 elements on the unit sphere using a Quasi-Monte Carlo method. Our goal is to calculate the probability of robust feasibility for this network and uncertain entry loads by using a spheric radial decomposition and applying Algorithm 1.The performance of the algorithm is investigated by benchmarking the algorithm on the given instance under a variety of parameter combinations. All experiments were carried out using GUROBI 7.5 [17] with 4 threads running on machines with Xeon E3-1240 v5 CPUs (4 cores, 3.5 GHz each).

We apply Algorithm 1 to all 10 000 rays using all combinations $\varepsilon \in \{2^{-6}, 2^{-5}, \ldots, 2^4\}$ of relaxation parameters and bisection termination tolerances $\mathrm{tol} \in \{0.001, 0.01, 0.1\}$. Experiments for smaller tolerances down to $\mathrm{tol} = 10^{-6}$ were carried out as well but are omitted here since they produced almost identical probabilities, when compared to $\mathrm{tol} = 10^{-3}$. The results of this study are displayed in Figure 3. The probabilities for robust feasibility of the exit nomination and the capacity extension of the instance are displayed in Figure 3a. We determine the overall probability to be between 78 % and 78.5 %, depending on ε and tol. As expected, we obtain more conservative solutions for increasing approximation parameters ε. However, the influence of ε is much smaller than expected, even for large ε. In the same fashion, increasing the bisection termination tolerances tol leads to more conservative solutions. We note that for both parameters, a combination of $\varepsilon = \frac{1}{2}$ and $\mathrm{tol} = 0.001$ produces solutions that can be improved only very little (within the scope of this study) by decreasing both parameters further. The overall running times for all rays, i.e. the cumulated running time of Algorithm (1), applied for each ray, are plotted in Figure 3b. As expected, the running times increase for decreasing parameter ε, as the latter leads to more complex MIP models. A decrease in tolerances tol leads to a

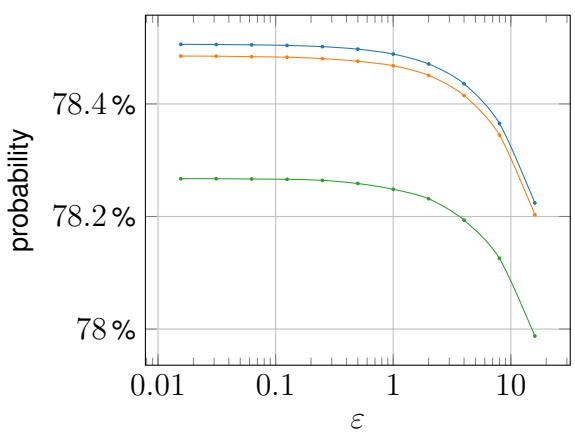

(a) Probability of robust feasibility as a function of relaxation quality ϵ.

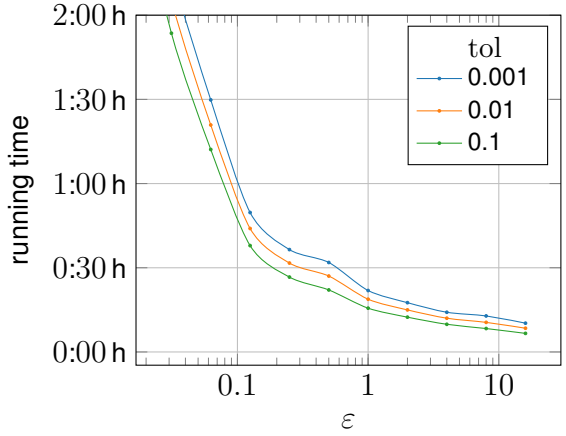

(b) Total running time for all rays as a function of bisection termination tolerance ϵ.

Figure 3: Resulting probability and total running time for 10 000 rays using different relaxation qualities ε and bisection termination tolerances tol.

larger number of iterations of the bisection algorithm and thus to longer running times as well.

In the previous experiments, we focused on the influence of the relaxation parameter ε and the bisection precision tolerance tol on the algorithm's running time and on the reliability of the obtained probability. Another important impact on the overall running time is the number of rays that needs to be used. Figure 4a shows the resulting probability when only the first k rays of the 10 000 given samples

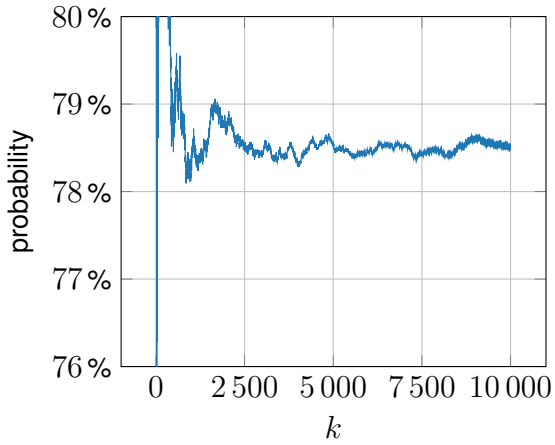

(a) Using up to 10 000 rays for the probability calculation.

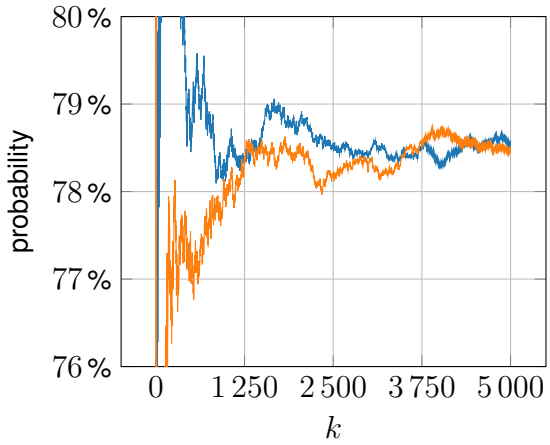

(b) Comparison between two collections of 5000 rays each.

Figure 4: Probability plot when using only the first k rays for its computation. Parameters used in ray length calculation: $\varepsilon = \frac{1}{2}$ and $\mathrm{tol} = 0.001$.

are used for the probability calculation. At a glance, we observe large fluctuations when using only up to about 2500 rays. A considerable decrease in the magnitude of the probability fluctuation can be seen for values of $k \geq 2500$. We further strengthen this observation in Figure 4b by comparing the first graph with a second graph that was obtained from 5000 other random sphere vectors in the same fashion. Since the second graph follows the same pattern, we conclude that for the instance considered here, the number of rays should not be smaller than 2500 if a reliable probability has to be calculated.

Assuming that the parameter selection $k = 2500$, $\varepsilon = \frac{1}{2}$, and $\mathrm{tol} = 0.001$ is sufficient for a reliable probability calculation, the sum of all MIP running times is about 8 min. We demonstrate the practical applicability of our method by solving a simple optimization task. The goal is to determine capacities for the two entry nodes such that the probability of robust feasibility is at least 75 %. We use a linear cost function with equal costs for expansion at each node. As it is unknown whether the star-shaped property holds for this instance, the calculated probabilities are all lower bounds to the true probability. In Section 3, the capacity problem with uncertain exit loads has been solved using (sub)gradient information in the sense of [2]. However, due to the different situation here caused by the MIP-approximations and the robust constraints, the derivation of suitable (sub)gradients needs further research that is beyond the scope of this article. Instead, we solve this optimization problem using a gradient free pattern search algorithm available in MATLAB [21]; see [6] for a general overview of derivative optimization. Figure 5 shows the steps of the algorithm displayed over level sets with different probabilities in different colors. Overall, the pattern search algorithm converged after 108 function evaluations and a total running time for all MIPs of about 6 h. On average, a function evaluation performed with our MIP-based approach took 3.5 min using the parameter selection from above. The gray circles represent extra function evaluations outside of the optimization trajectory. The black connected dots show the trajectory of the pattern search algorithm, with the optimum marked by a red cross.

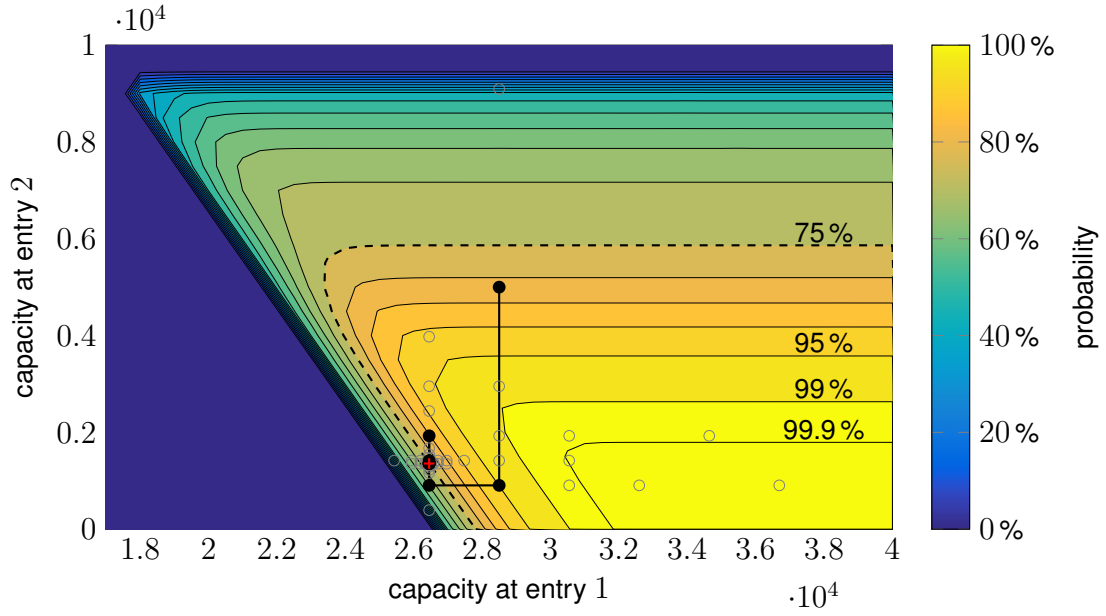

Figure 5: Contour plot of the probability for robust feasible entry capacities together with the trajectory of a gradient-free optimization method to determine a capacity with 75 % feasibility.

This concludes the discussion and presentation of the methodology for stationary gas networks. In the next section, transient systems controlled by the wave equation are discussed.

5 Stabilization with probabilistic constraints of a system governed by the wave equation

Now, we consider a transient system that is governed by the wave equation. The wave equation is a linear model of the gas flow in gas pipelines for sufficiently small velocities. The state is determined by an initial boundary value problem with Dirichlet boundary data at one end and Neumann boundary

feedback at the other end of the space interval. The initial data and the boundary data are given by a stochastic process. The aim is to maximize the probability to stay near a desired state everywhere in the time space domain.

Let a finite length $L > 0$ and a finite time $T > 0$ be given. In this section, let $\mathcal{U} = [0, T] \times [0, L]$. Let $c > 0$ denote the sound speed in the gas. Let a stationary velocity field $\bar{v}$ be given, see [15]. Let $v = \tilde{v} - \bar{v}$ denote the difference between the velocity and the stationary state. If the norm of $\bar{v}$ is sufficiently small, the dynamics for v are governed by the wave equation $v_{tt} = c^2\, v_{xx}$. Moreover the gas density ρ satisfies the wave equation $\rho_{tt} = c^2 \rho_{xx}$ and the flow rate q of the gas satisfies the wave equation $q_{tt} = c^2 q_{xx}$; see [16]. For given uncertain boundary data (that model the uncertain demand) $\xi \in L^\infty(0, T)$, an uncertain initial state $(v_0, v_1) \in L^\infty(0, L) \times L^1(0, L)$ and a feedback parameter $\eta > 0$, we consider the closed loop system that is governed by the initial boundary value problem for $(t,\, x) \in \mathcal{U}$

$$\begin{cases} v(0,\, x) = v_0(x), & v_t(0,\, x) = v_1(x), \\ v_x(t,\, 0) = \eta\, v_t(t,\, 0), & v(t,\, L) = \xi(t), \\ v_{tt}(t,\, x) = c^2 v_{xx}(t,\, x). & \end{cases} \tag{S}$$

An explicit representation of the generated state in terms of travelling waves (d'Alembert's solution) is given in [13], [14]. This allows the computation of the system state $v \in L^\infty(\mathcal{U})$ without discretization errors. In the operation of pipeline networks, there is a constraint on the magnitude of the flow velocity in the pipe. Let $v_{\max} > 0$ be an upper bound for the velocity. We consider the probabilistic constraint for the probability

$$\mathbb{P}\left(\|v\|_{L^\infty} \le v_{\max}\right) \tag{37}$$

where v solves (S) and $\|\cdot\|_{L^\infty}$ denotes the norm on $L^\infty(\mathcal{U})$.

In order to write the probabilistic constraint similar to (4), we introduce the notation

$$g(\tilde{v}, \xi, u) := v_{\max} - |\tilde{v}(u) - \bar{v}(u)|, \tag{38}$$

with $\xi = (a, b),\ a = (a_k)_{k=1}^N, b = (b_k)_{k=1}^N, u = (t, x) \in \mathcal{U}$, where $\tilde{v}$ solves the initial boundary value problem (S) with initial and boundary data that depend on the parameter (a, b) (see (KL-id) and (KL-bd) below).

Theorem 2 (Solution of system (S))**.**
Consider system (S) *with* $\xi \in L^\infty(0, T)$ *and* $(v_0, v_1) \in L^\infty(0, L) \times L^1(0, L)$ *for the feedback parameter* $\eta = \frac{1}{c}$. *Define the antiderivative of* v_1 *by*

$$V_1(x) := \int_0^x v_1(s)\, \mathrm{d}s$$

and define for

$$\alpha(s) := \begin{cases} v_0(cs) + \frac{1}{c} V_1(cs) & \text{for } s \in \left[0, \frac{L}{c}\right) \\ 2\xi\left(s - \frac{L}{c}\right) - \beta\left(s - \frac{L}{c}\right) & \text{for } s \in \left[\frac{L}{c}, T + \frac{L}{c}\right] \end{cases}$$

and

$$\beta(s) := \begin{cases} v_0(L - cs) - \frac{1}{c} V_1(L - cs) & \text{for } s \in \left[0, \frac{L}{c}\right) \\ v_0(0) & \text{for } s \in \left[\frac{L}{c}, T + \frac{L}{c}\right]. \end{cases}$$

Then the function

$$v(t, x) := \tfrac{1}{2}\alpha\left(t + \tfrac{x}{c}\right) + \tfrac{1}{2}\beta\left(t + \tfrac{L - x}{c}\right) \tag{39}$$

solves system (S) *and the solution* v *lies in* $L^\infty(\mathcal{U})$.

Proof. We show that v defined in (39) fulfills the pde. First we see that v satisfies the wave equation, because we have

$$\begin{aligned} v_{tt} &= \tfrac{1}{2}\alpha''\left(t+\tfrac{x}{c}\right) + \tfrac{1}{2}\beta''\left(t+\tfrac{L-x}{x}\right) \\ v_{xx} &= \tfrac{1}{2c^2}\alpha''\left(t+\tfrac{x}{c}\right) + \tfrac{1}{2c^2}\beta''\left(t+\tfrac{L-x}{c}\right). \end{aligned}$$

Now we show that v satisfies the initial conditions. At $t=0$, we have for all $x \in (0,L)$

$$\begin{aligned} v(0,x) &= \tfrac{1}{2}\alpha\left(\tfrac{x}{c}\right) + \tfrac{1}{2}\beta\left(\tfrac{L-x}{c}\right) \\ &= \tfrac{1}{2}\left[v_0(x) + \tfrac{1}{c}V_1(x)\right] + \tfrac{1}{2}\left[v_0(x) - \tfrac{1}{c}V_1(x)\right] = v_0(x). \end{aligned}$$

For the time derivative at $t=0,\ x \in (0,L)$ we have

$$\begin{aligned} v_t(0,x) &= \tfrac{1}{2}\alpha'\left(\tfrac{x}{c}\right) + \tfrac{1}{2}\beta'\left(\tfrac{L-x}{c}\right) \\ &= \tfrac{1}{2}\left[v_0'(x) + v_1(x)\right] - \tfrac{1}{2}\left[v_0'(x) - v_1(x)\right] = v_1(x), \end{aligned}$$

where the derivatives are to be understood in the sense of distributions. Finally, we show that the boundary conditions are fulfilled. Now, we proove that the Dirichlet boundary condition at $x = L$ is fulfilled for $t > 0$. We have

$$v(t,L) = \tfrac{1}{2}\alpha(t+\tfrac{L}{c}) + \tfrac{1}{2}\beta(t) = \tfrac{1}{2}[2\xi(t) - \beta(t)] + \tfrac{1}{2}\beta(t) = \xi(t).$$

For the feedback law at $x = 0$, we have

$$\begin{aligned} v_x(t,0) &= \tfrac{1}{2c}\alpha'(t) - \tfrac{1}{2c}\beta'(t+\tfrac{L}{c}) = \tfrac{1}{2c}\alpha'(t) - \tfrac{1}{2c}v_0'(0) \\ \eta v_t(t,0) &= \tfrac{\eta}{2}\alpha'(t) - \tfrac{\eta}{2}\beta'(t+\tfrac{L}{c}) \ \ = \tfrac{1}{2c}\alpha'(t) - \tfrac{1}{2c}v_0'(0). \end{aligned}$$

Now we show that v lies in $L^\infty(\mathcal{U})$. By the assumptions, we have $v_0 \in L^\infty(0,L)$ and $\xi \in L^\infty(0,L)$. The claim is true if V_1 is in $L^\infty(0,L)$. We know that v_1 is in $L^1(0,L)$. This implies

$$\|V_1\|_{L^\infty} = \operatorname*{ess\,sup}_{x\in(0,L)} \left| \int_0^x v_1(s)\,\mathrm{d}s \right| \leq \operatorname*{ess\,sup}_{x\in(0,L)} \int_0^x |v_1(s)|\,\mathrm{d}s \leq \int_0^L |v_1(s)|\,\mathrm{d}s = \|v_1\|_{L^1}.$$

This finishes the proof Theorem 2. □

Theorem 3 (Value of $\|v\|_{L^\infty}$ in terms of initial and boundary data)**.** *Let v be a solution of system* (S) *under the assumptions of Theorem 2. For $(t,x) \in \mathcal{U}$, define*

$$\begin{aligned} m_1(t,x) &:= \tfrac{1}{2}\left[v_0(x+ct) + \tfrac{1}{c}V_1(x+ct)\right] + \tfrac{1}{2}\left[v_0(x-ct) - \tfrac{1}{c}V_1(x-ct)\right], \\ m_2(t,x) &:= \tfrac{1}{2}\left[v_0(ct+x) + \tfrac{1}{c}V_1(ct+x) + v_0(0)\right], \\ m_3(t,x) &:= \xi\left(t+\tfrac{x-L}{c}\right) + \tfrac{1}{2}\left[v_0(ct+x) - \tfrac{1}{c}V_1(ct+x) - \right. \\ &\qquad \left. v_0(2L-x-ct) + \tfrac{1}{c}V_1(2L-x-ct)\right], \\ m_4(t,x) &:= \xi(t+\tfrac{x-L}{c}) + \tfrac{1}{2}\left[\tfrac{1}{c}V_1(2L-x-ct) + v_0(0) - v_0(2L-x-ct)\right], \\ m_5(t,x) &:= \xi(t+\tfrac{x-L}{c}). \end{aligned}$$

Set

$$\begin{aligned} \Omega_1 &:= \left\{(t,x) \in \mathcal{U} \mid t < \min\{\tfrac{L-x}{c}, \tfrac{x}{c}\}\right\}, \\ \Omega_2 &:= \left\{(t,x) \in \mathcal{U} \mid \tfrac{x}{c} \leq t < \tfrac{L-x}{c}\right\}, \\ \Omega_3 &:= \left\{(t,x) \in \mathcal{U} \mid \tfrac{L-x}{c} \leq t < \tfrac{x}{c}\right\}, \\ \Omega_4 &:= \left\{(t,x) \in \mathcal{U} \mid \max\{\tfrac{L-x}{c}, \tfrac{x}{c}\} \leq t < \tfrac{L}{c} + \tfrac{L-x}{c}\right\}, \\ \Omega_5 &:= \left\{(t,x) \in \mathcal{U} \mid t \geq \tfrac{L}{c} + \tfrac{L-x}{c}\right\} \end{aligned}$$

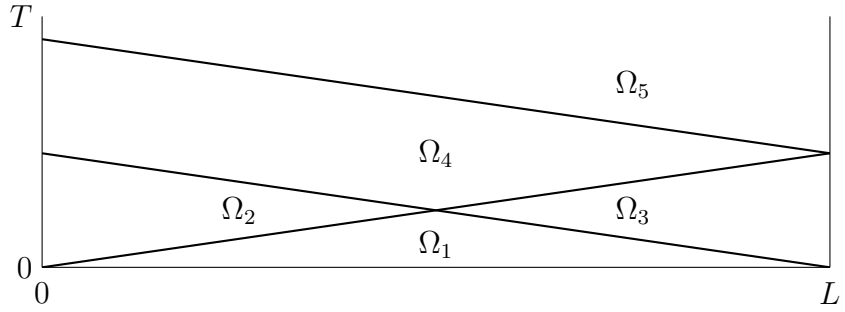

Figure 6: Decomposition of the space-time domain $\mathcal{U}$

(see Fig. 6). Furthermore, for $i \in \{1, \dots, 5\}$, *set*

$$M_i := \sup\{|m_i(t,x)| \colon (t,x) \in \Omega_i\}.$$

Then the L^∞*-norm of the velocity* v *is given by*

$$\|v\|_{L^\infty} = \max\{M_1, M_2, M_3, M_4, M_5\}.$$

Proof. By Theorem 2 the solution of system (S) is given by

$$v(t,x) := \tfrac{1}{2}\alpha\left(t + \tfrac{x}{c}\right) + \tfrac{1}{2}\beta\left(t + \tfrac{L-x}{c}\right).$$

By the definition of α and β, there are four cases to consider. The last case is split into two subcases. The first case $t < \min\left\{\frac{x}{c}, \frac{L-c}{c}\right\}$ is the first case for both α and β. We have

$$v(t,x) = \tfrac{1}{2}\left[v_0(x+ct) + \tfrac{1}{c}V_1(x+ct)\right] + \tfrac{1}{2}\left[v_0(x-ct) - \tfrac{1}{c}V_1(x-ct)\right].$$

For $\frac{x}{c} \le t < \frac{L-x}{c}$, we are in the first case for α and in the second case for β. Note that the interval for t can only be nonempty for $x \in (0, \frac{L}{2})$. We have

$$v(t,x) = \tfrac{1}{2}\left[v_0(ct+x) + \tfrac{1}{c}V_1(ct+x) + v_0(0)\right].$$

For $\frac{L-x}{c} \le t < \frac{x}{c}$, we are in the second case for α and in the first case for β. Note that the interval for t can only be nonempty for $x \in (\frac{L}{2}, L)$. Since $t < \frac{x}{c} < \frac{L}{c}$ and $\frac{x-L}{c} < 0$, we have $t + \frac{x-L}{c} < \frac{L}{c}$ and therefore

$$\begin{aligned} v(t,x) &= \tfrac{1}{2}\left[2\xi(t+\tfrac{x-L}{c}) - \beta(t+\tfrac{x-L}{c}) + \beta(t+\tfrac{L-x}{c})\right] \\ &= \xi(t+\tfrac{x-L}{c}) - \tfrac{1}{2}\beta(t+\tfrac{x-L}{c}) + \tfrac{1}{2}\left[v_0(ct+x) - \tfrac{1}{c}V_1(ct+x)\right] \\ &= \xi(t+\tfrac{x-L}{c}) - \tfrac{1}{2}\left[v_0(2L-x-ct) - \tfrac{1}{c}V_1(2L-x-ct)\right] \\ &\quad + \tfrac{1}{2}\left[v_0(ct+x) - \tfrac{1}{c}V_1(ct+x)\right]. \end{aligned}$$

The last case to consider is $t \ge \max\{\frac{L-x}{c}, \frac{x}{c}\}$. It leads to

$$\begin{aligned} &v(t,x) = \tfrac{1}{2}\left[2\xi(t+\tfrac{x-L}{c}) - \beta(t+\tfrac{x-L}{c}) + v_0(0)\right] = \\ &\begin{cases} \xi(t+\frac{x-L}{c}) + \frac{1}{2}\left[\frac{1}{c}V_1(2L-x-ct) + v_0(0) - v_0(2L-x-ct)\right], & t < \frac{L}{c} + \frac{L-x}{c} \\ \xi(t+\frac{x-L}{c}), & t \ge \frac{L}{c} + \frac{L-x}{c}. \end{cases} \end{aligned}$$

This yields the assertion of Thm. 3. □

5.1 Boundary data with random amplitude, frequency and phaseshift

For the boundary data, we consider the parametric family

$$\xi(t) := \lambda \cos(\omega t + \kappa) \tag{cos-bd}$$

with a random variable $(\lambda,\ \kappa,\ \omega)$ and the compatible initial data

$$v_0(x) = \lambda \cos(\kappa), \quad v_1 = 0. \tag{cos-id}$$

We assume that $(\lambda,\ \kappa,\ \omega)$ is normally distributed with expected value $\mu \in \mathbb{R}^3$ and a positive definite covariance matrix $\Sigma \in \mathbb{R}^{3\times 3}$. For the numerical computation of the probability, we use the spheric radial decomposition described in Section 3.2.

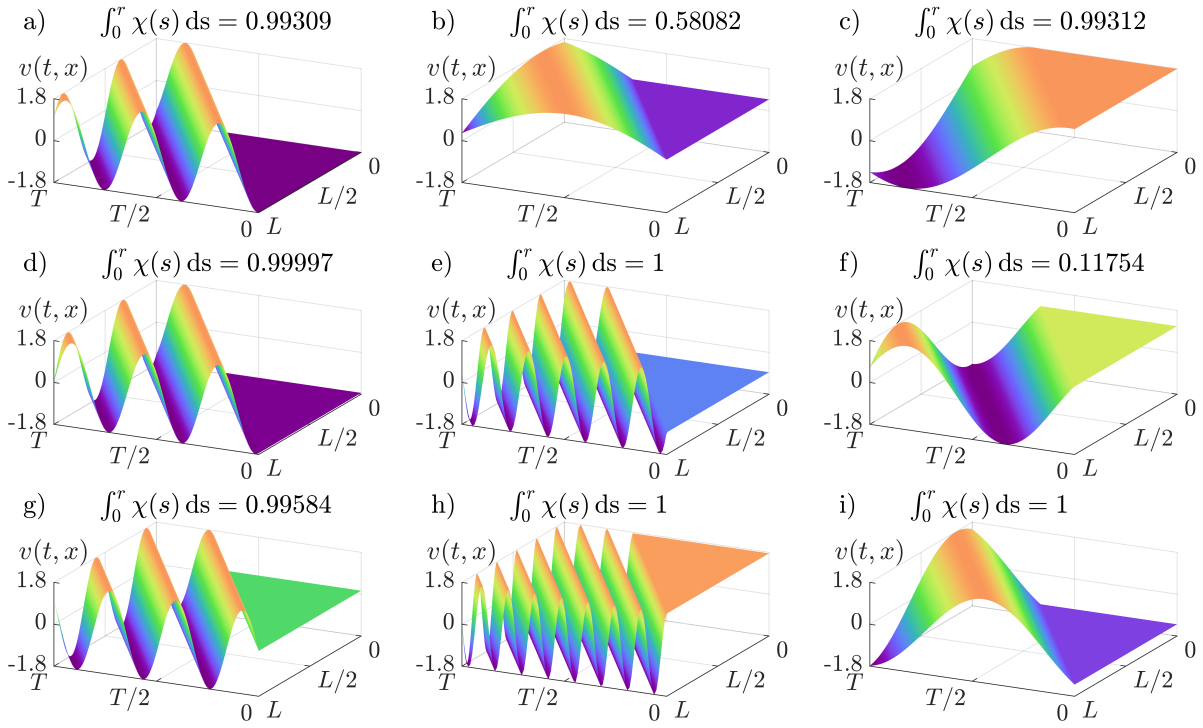

Figure 7: The solution v of the wave equation for nine samples $(\lambda, \omega, \kappa)$ on the sphere. The radius r is scaled such that $\|v\|_{L^\infty} = v_{\max}$ holds. The value of the cumulative distribution of the chi distribution evaluated at this radius is given on top of each picture. The probability for the solution to be bounded by $v^{\max}$ is $\mathbb{P}\left(\|v\|_{L^\infty} \leq v^{\max}\right) \approx 0.7856$ for the data $T = 6$, $L = 2$, $c = 0.5$, $v^{\max} = 1.8$. The random vector $(\lambda, \omega, \kappa)$ is normal distributed with expected value $\mu = (1, 1, 1)$ and covariance matrix $\Sigma = I$. The number of samples used to approximate the probability is 20000.

Corollary 1 (Analytic formula for $\|v\|_{L^\infty}$)**.** *Let v be a solution of system* (S) *under the assumptions of Theorem 2 for the initial conditions given by* (cos-id) *and the Dirichlet boundary data at $x = L$ given by* (cos-bd)*. Then*

$$\|v\|_{L^\infty} \leq |\lambda|.$$

Proof. With the definitions from Theorem 3 and (cos-bd) as well as (cos-id), we have

$$\begin{aligned}
m_1(t,x) &:= v_0(ct+x) = \lambda\cos(\kappa),\\
m_2(t,x) &:= \tfrac{1}{2}\left[v_0(ct+x) + \tfrac{1}{c}V_1(ct+x) + v_0(0)\right] = \lambda\cos(\kappa),\\
m_3(t,x) &:= \xi\left(t+\tfrac{x-L}{c}\right) + \tfrac{1}{2}\left[v_0(ct+x) - \tfrac{1}{c}V_1(ct+x) - \right.\\
&\qquad \left. v_0(2L-x-ct) + \tfrac{1}{c}V_1(2L-x-ct)\right]\\
&= \lambda\,\cos\left(\omega\left(t+\tfrac{x-L}{c}\right)+\kappa\right)\\
m_4(t,x) &:= \xi(t+\tfrac{x-L}{c}) + \tfrac{1}{2}\left[\tfrac{1}{c}V_1(2L-x-ct) + v_0(0) - v_0(2L-x-ct)\right]\\
&= \lambda\,\cos\left(\omega\left(t+\tfrac{x-L}{c}\right)+\kappa\right).\\
m_5(t,x) &:= \xi(t+\tfrac{x-L}{c}) = \lambda\,\cos\left(\omega\left(t+\tfrac{x-L}{c}\right)+\kappa\right)
\end{aligned}$$

By $|m_i(t,x)| \le |\lambda|$ for $i = 1,\dots,5$ the claim follows. □

Remark. *If $\omega \neq 0$ and T is sufficiently large, then $\|v\|_\infty = |\lambda|$ holds.*

5.2 Karhunen-Loève approximation of a Wiener process as initial and boundary data

We consider the Karhunen-Loève representation (see [19]) of a Wiener process on $[0,T]$ with covariance function $\mathrm{Cov}(W_t, W_s) = \min(s,t)$ given by

$$W_t = \sqrt{2T}\sum_{k=1}^{\infty} a_k \frac{\sin\left(\omega_k \pi \frac{t}{T}\right)}{\omega_k \pi}, \quad \omega_k = k - \tfrac{1}{2},$$

with independently normally distributed random variables a_k. It is reasonable to use a finite approximation of it as boundary data, i.e.

$$\xi(t) = \sqrt{2T}\sum_{k=1}^{N} a_k \frac{\sin\left(\omega_k \pi \frac{t}{T}\right)}{\omega_k \pi}, \quad \omega_k = k - \tfrac{1}{2}, \text{ on } [0,T]. \tag{KL-bd}$$

Analogously, we choose the compatible initial data

$$v_0(x) = \sqrt{2L}\sum_{k=1}^{N} b_k \frac{\sin\left(\omega_k \pi \frac{L-x}{L}\right)}{\omega_k \pi}, \quad \omega_k = k - \tfrac{1}{2}, \text{ on } [0,L], \tag{KL-id}$$

with independently normally distributed random variables b_k. We have the compatibility condition $\xi(0) = v_0(L) = 0$. Furthermore, set $v_1 = 0$. Different realizations of the initial and boundary data can be seen in Figures 8 and 9. The solution of the wave equation for different realizations of the initial and boundary data is depicted in Figure 10.

The case is much more involved than that in Section 5.1, since the value of $\|v\|_{L^\infty}$ is not easily expressed as an analytic function of the random variables. This means a sampling scheme based on spheric radial decomposition can not be directly be applied. We use a quasi Monte Carlo method based on a Sobol sequence instead.

If one wants to approximate the L^∞- norm of the velocity by pointwise evaluation on a grid, Lipschitz continuity of the velocity is required.

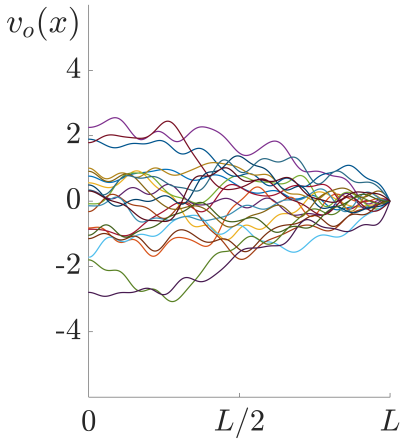

Figure 8: Different realizations (21) of the initial data for a Karhunen-Loève sum with 20 standard normally distributed coefficients

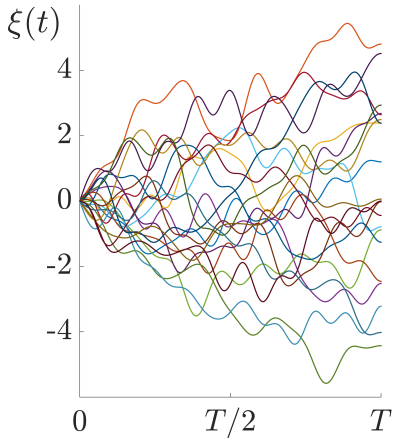

Figure 9: Different realizations (21) of the boundary data for a Karhunen-Loève sum with 20 standard normally distributed coefficients

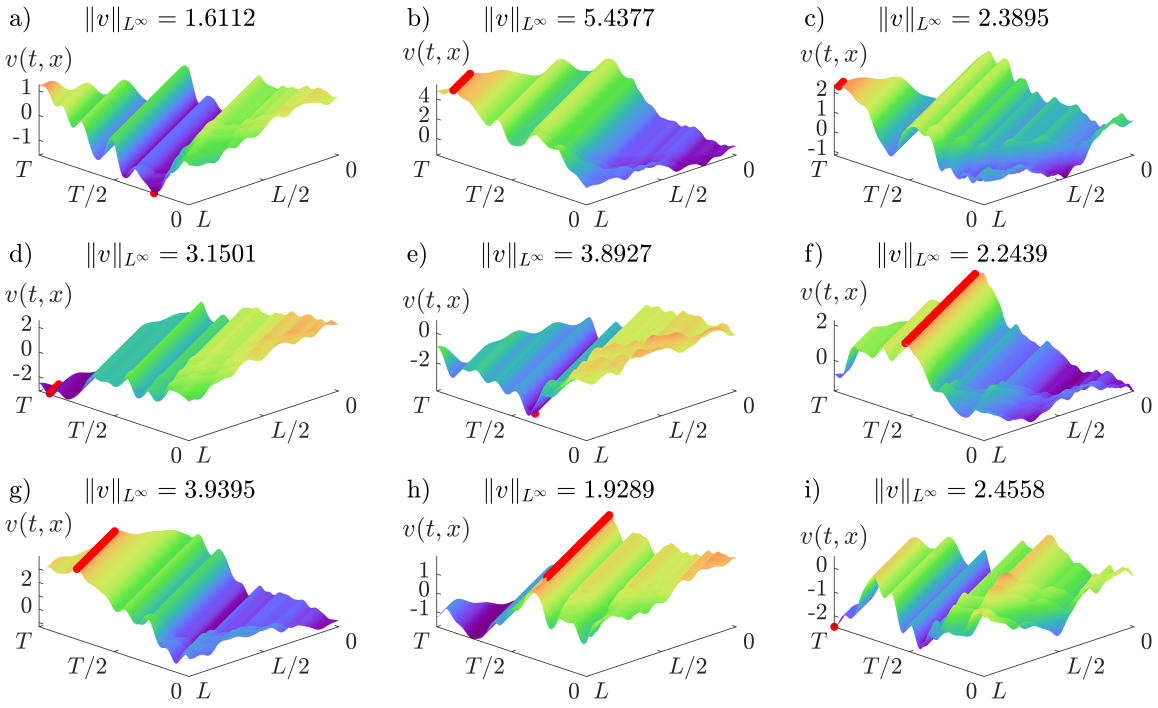

Figure 10: The solution v of the wave equation with boundary and initial data given by the functions in (KL-bd) and (KL-id) for nine samples of the standard normal distributed random vector (a, b) with realizations in $\mathbb{R}^{40}$, i.e., $N = 20$. The constants $T = 6, L = 2, c = 0.5$ were used. The bound $v_{\max} = 5$ was chosen and $\bar{v} = 0$ was used. The probability of $\|v + \bar{v}\|_{L^\infty} \leq v_{\max}$ is 0.8808 with 10000 samples used. The value of the L^∞-norm is approximated by evaluation on a 100×100 grid on $\mathcal{U}$. The points, where the value of the L^∞- norm is attained are marked with a point.

Theorem 4 (Lipschitz continuity of the solution)**.** *Assume the boundary data $\xi \in \mathcal{C}^{0,1}(0,T)$ and initial data $v_0 \in \mathcal{C}^{0,1}(0,L)$ to be Lipschitz continuous and assume that Lipschitz compatibility over the edge holds, i.e. that we have*

$$|\xi(t) - v_0(L-x)| \le K|t - L + x|, \quad \textit{for} \quad (t,x) \in \mathcal{U} \tag{40}$$

with a Lipschitz constant $K > 0$. Furthermore, let $v_1 \in L^\infty(0,L)$.
Then, under the assumptions of Thm. 2, the solution v of system (S) *is Lipschitz continuous on $\mathcal{U}$, i.e., $v \in \mathcal{C}^{0,1}(\mathcal{U})$.*

Proof. The sum of Lipschitz continuous functions is Lipschitz continuous. It is therefore sufficient to show the Lipschitz continuity of α and β defined as in Theorem 2. Without loss of generality–by going to the maximum of the occurring Lipschitz constants–we assume that they are all the same and denote each of them by $K > 0$. First, we show the Lipschitz continuity of V_1. We have, for $x, y \in [0, L]$

$$\begin{aligned} |V(x) - V(y)| &= \left| \int_0^x v_1(s)\,\mathrm{d}s - \int_0^y v_1(s)\,\mathrm{d}s \right| = \left| \int_y^x v_1(s)\,\mathrm{d}s \right| \\ &\le |x-y|\,\|v_1\|_{L^\infty} \le K|x-y|. \end{aligned}$$

The Lipschitz continuity of β is clear in the individual intervals $\left[0, \frac{L}{c}\right)$ and $\left[\frac{L}{c}, T + \frac{L}{c}\right)$. Consider $s \in \left[0, \frac{L}{c}\right)$ and $r \in \left[\frac{L}{c}, T + \frac{L}{c}\right)$. Then, using $V_1(0) = 0$ and $\left|\frac{L}{c} - s\right| = \frac{L}{c} - s \le r - s = |r - s|$, leads to

$$\begin{aligned} |\beta(s) - \beta(r)| &= \tfrac{1}{c}|cv_0(L - cs) - V_1(L - cs) - cv_0(0) + V_1(0)| \\ &\le \tfrac{K}{c}|L - cs| \le K|r - s|. \end{aligned}$$

The Lipschitz continuity of β of ξ imply that α is Lipschitz on $t \ge \frac{L}{c}$ and by the Lipschitz continuity of v_0 and V_1 it is Lipschitz on $\left[0, \frac{L}{c}\right)$. Again, the case $s \in \left[0, \frac{L}{c}\right)$ and $r \ge \frac{L}{c}$ is remaining. We obtain

$$|\alpha(s) - \alpha(r)| = \left|v_0(cs) + \tfrac{1}{c}V_1(cs) - 2\xi\left(r - \tfrac{L}{c}\right) + \beta\left(r - \tfrac{L}{c}\right)\right|.$$

For $\frac{L}{c} \le r < \frac{2L}{c}$, this yields by the definition of β

$$\begin{aligned} |\alpha(s) - \alpha(r)| &= \left|v_0(cs) + \tfrac{1}{c}V_1(cs) - 2\xi\left(r - \tfrac{L}{c}\right) + v_0(2L - cr) - \tfrac{1}{c}V_1(2L - cr)\right| \\ &= \Big|v_0(cs) - v_0(L) + 2(v_0(L) - \xi\left(r - \tfrac{L}{c}\right)) \\ &\quad + v_0(2L - cr) - v_0(L) + \tfrac{1}{c}\left(V_1(cs) - V_1(2L - cr)\right)\Big|. \end{aligned}$$

By the triangle inequality and the compatibility $v_0(L) = \xi(0)$, we obtain

$$\begin{aligned} |\alpha(s) - \alpha(r)| &\le |v_0(cs) - v_0(L)| + 2\left|\xi(0) - \xi\left(r - \tfrac{L}{c}\right)\right| \\ &\quad + |v_0(2L - cr) - v_0(L)| + \tfrac{1}{c}|V_1(cs) - V_1(2L - cr)| \\ &\le K|cs - L| + 2K\left|-r + \tfrac{L}{c}\right| + K|L - cr| \\ &\quad + \tfrac{K}{c}|cs - L| + \tfrac{K}{c}|-L + cr| \\ &= K\left[L - cs + 2(r - \tfrac{L}{c}) + cr - L + \tfrac{L}{c} - s + r - \tfrac{L}{c}\right] \\ &\le K\left[c(r-s) + 2(r-s) + (r-s)\right] = K(c+3)|r-s|, \end{aligned}$$

since $-\frac{L}{c} \leq -s$. For $r \geq \frac{2L}{c}$, we have by the definition of β and $V_1(0) = 0$

$$\begin{aligned}
|\alpha(s) - \alpha(r)| &= \left|v_0(cs) + \tfrac{1}{c}V_1(cs) - 2\xi\left(r - \tfrac{L}{c}\right) + v_0(0)\right| \\
&= |v_0(cs) - v(L) + 2\left(v_0(L) - \xi\left(r - \tfrac{L}{c}\right)\right) + v_0(0) \\
&\quad - v_0(L) + \tfrac{1}{c}V_1(cs) - \tfrac{1}{c}V_1(0)| \\
&\leq |v_0(cs) - v(L)| + 2\left|\xi(0) - \xi\left(r - \tfrac{L}{c}\right)\right| \\
&\quad + |v_0(0) - v_0(L)| + \tfrac{1}{c}|V_1(cs) - V_1(0)| \\
&\leq K|cs - L| + 2K\left|-r + \tfrac{L}{c}\right| + K|L| + \tfrac{K}{c}|cs| \\
&= K\left[L - cs + 2(r - \tfrac{L}{c}) + L + s\right] \\
&\leq K\left[c(r-s) + 2(r-s) + (r-s)\right] \leq K(c+3)|r-s|,
\end{aligned}$$

because $2L \leq rc$, $-\frac{L}{c} \leq -s$ and $r - s \geq \frac{2L}{c} - s \geq \frac{L}{c} \geq s$. This shows the Lipschitz continuity of α and concludes the proof. □

Remark. *Also for general feedback gains $\eta > 0$, results similar to Thm. 2 and Thm. 4 hold.*

5.3 Optimization of the feedback parameter

The feedback parameter η can be chosen such that the probability (37) as a function of η is maximized. We call this function $G(\eta)$. We consider the probability to stay under the bound $v_{\max} = 5$ for different feedback parameters $\eta > 0$ on a grid with stepsize 0.05 between 1.5 and 4. The data for the

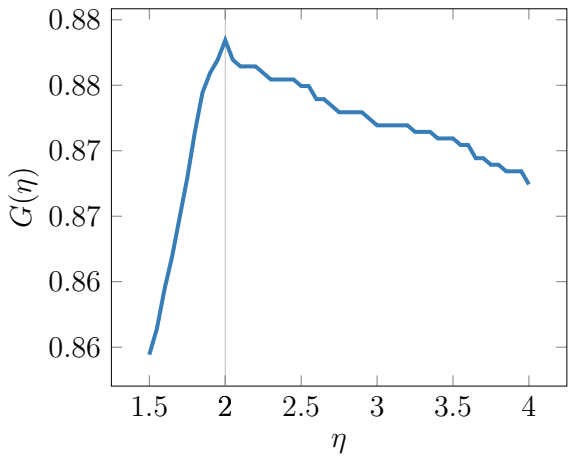

Figure 11: The probability to stay under the bound $v_{\max} = 5$ over the feedback parameter η for the data $L = 2$, $c = 0.5$, $T = 2$ using 2000 samples. The maximum of the probability is reached for completely absorbing feedback $\eta = 1/c = 2$.

example has been chosen as $L = 2$, $T = 2$, $c = 0.5$. For the approximation of the probability, 2000 samples were used for each value of η. The maximum of the probability is reached for completely absorbing feedback $\eta = 1/c = 2$. The peak in probability is very distinct. At the peak the probability function appears to be nonsmooth. Numerically, we find that the choice $\eta = 1/c$ is optimal; see Fig. 11.

6 Conclusion

In this paper we introduced a joint model of probabilistic and robust constraints, so-called probust constraints and illustrated their importance for gas transport under uncertainty. In particular, we addressed the problem of capacity maximization under uncertainty thereby distinguishing between the cases of uncertain exit and uncertain entry loads. Moreover, we considered a stabilization problem in a transient system governed by the wave equation and subject to probust constraints. By applying the spheric radial decomposition of Gaussian random vectors, we approximated the occurring probabilities and–where possible–their sensitivities with respect to the decision variables in order to numerically solve the resulting optimization problems. There are a lot of remaining challenges for future work, such as efficient incorporation of cycles or active elements in the network. Moreover, a full integration of the methodology outlined in Section 4 for the robust treatment of uncertain entries with the capacity maximization problem described in Section 3 ultimately would allow an application of the probust approach to arbitrary network topologies.

References

[1] van Ackooij, W., Frangioni, A., de Oliveira, W.: Inexact stabilized Benders' decomposition approaches with application to chance-constrained problems with finite support. Computational Optimization and Applications **65**(3), 637–669 (2016). DOI 10.1007/s10589-016-9851-z

[2] v. Ackooij, W., Henrion, R.: (Sub-) gradient formulae for probability functions of random inequality systems under Gaussian distribution. SIAM/ASA Journal on Uncertainty Quantification **5**, 63–87 (2017). DOI 10.1137/16M1061308

[3] Aßmann, D., Liers, F., Stingl, M.: Decomposable robust two-stage optimization: An application to gas network operations under uncertainty (2017). Preprint SFB TRR 154, `https://opus4.kobv.de/opus4-trr154/frontdoor/index/index/docId/209`, Submitted for publication

[4] Ben-Tal, A., El Ghaoui, L., Nemirovski, A.: Robust Optimization. Princeton Series in Applied Mathematics. Princeton University Press (2009)

[5] Brauchart, J., Saff, E., Sloan, I., Womersley, R.: QMC designs: optimal order Quasi Monte Carlo integration schemes on the sphere. Mathematics of computation **83**(290), 2821–2851 (2014)

[6] Conn, A.R., Scheinberg, K., Vicente, L.N.: Introduction to Derivative-Free Optimization. SIAM, Philadelphia, PA, USA (2009)

[7] Dentcheva, D., Ruszczyński, A.: Robust stochastic dominance and its application to risk-averse optimization. Mathematical Programming **123**, 85–100 (2010)

[8] Geißler, B., Martin, A., Morsi, A., Schewe, L.: Using piecewise linear functions for solving MINLPs. In: J. Lee, S. Leyffer (eds.) Mixed Integer Nonlinear Programming, *The IMA Volumes in Mathematics and its Applications*, vol. 154, pp. 287–314. Springer New York Dordrecht Heidelberg London (2012)

[9] Genz, A., Bretz, F.: Computation of multivariate normal and t-probabilities, vol. 195. Springer (2009)

[10] Gotzes, C., Heitsch, H., Henrion, R., Schultz, R.: On the quantification of nomination feasibility in stationary gas networks with random load. Mathematical Methods of Operations Research **84**, 427–457 (2016). DOI 10.1007/s00186-016-0564-y

[11] Gotzes, C., Nitsche, S., Schultz, R.: Probability of feasible loads in passive gas networks with up to three cycles (2017). URL https://opus4.kobv.de/opus4-trr154/frontdoor/index/index/docId/135. Preprint SFB TRR 154, https://opus4.kobv.de/opus4-trr154/frontdoor/index/index/docId/135, Submitted for publication

[12] Grandón, T.G., Heitsch, H., Henrion, R.: A joint model of probabilistic/robust constraints for gas transport management in stationary networks. Computational Management Science **14**, 443–460 (2017). DOI 10.1007/s10287-017-0284-7

[13] Gugat, M.: Optimal Boundary Control and Boundary Stabilization of Hyperbolic Systems. Birkhäuser Basel (2015)

[14] Gugat, M., Leugering, G.: L^∞-norm minimal control of the wave equation: on the weakness of the bang-bang principle. ESAIM: COCV **14**(2), 254–283 (2008). DOI 10.1051/cocv:2007044

[15] Gugat, M., Leugering, G., Wang, K.: Neumann boundary feedback stabilization for a nonlinear wave equation: A strict H^2-Lyapunov function. Mathematical Control and Related Fields **7**(3), 419–448 (2017). DOI 10.3934/mcrf.2017015

[16] Gugat, M., Steffensen, S.: Dynamic boundary control games with networks of strings. COCV (2018). 10.1051/cocv/2017082

[17] Gurobi Optimization, Inc.: Gurobi optimizer reference manual (2016). URL http://www.gurobi.com

[18] Heitsch, H.: On probabilistic capacity maximization in a stationary gas network. WIAS Preprint no. 2540 (2018)

[19] Karhunen, K.: Über lineare Methoden in der Wahrscheinlichkeitsrechnung. Universitat Helsinki (1947)

[20] Koch, T., Hiller, B., Pfetsch, M.E., Schewe, L. (eds.): Evaluating Gas Network Capacities. SIAM-MOS series on Optimization. SIAM (2015)

[21] The Mathworks, Inc., Natick, Massachusetts: MATLAB version 9.1.0.441655 (R2016b) (2016)

[22] Montes, A., Wibmer, M.: Gröbner bases for polynomial systems with parameters. Journal of Symbolic Computation **45**(12), 1391 – 1425 (2010). DOI https://doi.org/10.1016/j.jsc.2010.06.017. URL http://www.sciencedirect.com/science/article/pii/S0747717110000970

[23] Padberg, M.: Approximating separable nonlinear functions via mixed zero-one programs. Operations Research Letters **27**(1), 1 – 5 (2000). DOI https://doi.org/10.1016/S0167-6377(00)00028-6. URL http://www.sciencedirect.com/science/article/pii/S0167637700000286

[24] Prékopa, A.: Stochastic programming. Springer Science & Business Media (1995). DOI 10.1007/978-94-017-3087-7

[25] Vázquez, F.G., Rückmann, J.J., Stein, O., Still, G.: Generalized semi-infinite programming: A tutorial. Journal of Computational and Applied Mathematics **217**(2), 394–419 (2008). DOI 10.1016/j.cam.2007.02.012. Special Issue: Semi-infinite Programming (SIP)

[26] Zymler, S., Kuhn, D., Rustem, B.: Distributionally robust joint chance constraints with second-order moment information. Mathematical Programming **137**, 167–198 (2013)